7. Chang, C.S., Kokontis, J. & Liao, S.T. Molecular cloning of human and rat complementary DNA encoding androgen receptors. *Science* **240**, 324–326 (1988).
8. Heinlein, C.A. & Chang, C. Androgen receptor in prostate cancer. *Endocr. Rev.* **25**, 276–308 (2004).
9. Yeh, S. & Chang, C. Cloning and characterization of a specific coactivator, ARA70, for the androgen receptor in human prostate cells. *Proc. Natl. Acad. Sci. USA* **93**, 5517–5521 (1996).
10. Heinlein, C.A. & Chang, C. Androgen receptor (AR) coregulators: an overview. *Endocr. Rev.* **23**, 175–200 (2002).
11. McCampbell, A. & Fischbeck, K.H. Polyglutamine and CBP: fatal attraction? *Nat. Med.* **7**, 528–530 (2001).
12. Sherman, M.Y. & Goldberg, A.L. Cellular defenses against unfolded proteins: a cell biologist thinks about neurodegenerative diseases. *Neuron* **29**, 15–32 (2001).
13. Ross, C.A. Polyglutamine pathogenesis: emergence of unifying mechanisms for Huntington's disease and related disorders. *Neuron* **35**, 819–822 (2002).
14. Merry, D.E., Kobayashi, Y., Bailey, C.K., Taye, A.A. & Fischbeck, K.H. Cleavage, aggregation and toxicity of the expanded androgen receptor in spinal and bulbar muscular atrophy. *Hum. Mol. Genet.* **7**, 693–701 (1998).
15. Tarlac, V. & Storey, E. Role of proteolysis in polyglutamine disorders. *J. Neurosci. Res.* **74**, 406–416 (2003).
16. Mandrusiak, L.M. *et al.* Transglutaminase potentiates ligand-dependent proteasome dysfunction induced by polyglutamine-expanded androgen receptor. *Hum. Mol. Genet.* **12**, 1497–1506 (2003).
17. Beauchemin, A.M. *et al.* Cytochrome c oxidase subunit Vb interacts with human androgen receptor: a potential mechanism for neurotoxicity in spinobulbar muscular atrophy. *Brain Res. Bull.* **56**, 285–297 (2001).
18. Katsuno, M. & Sobue, G. Polyglutamine diminishes VEGF; passage to motor neuron death? *Neuron* **41**, 677–679 (2004).
19. Katsuno, M. *et al.* Leuprorelin rescues polyglutamine-dependent phenotypes in a transgenic mouse model of spinal and bulbar muscular atrophy. *Nat. Med.* **9**, 768–773 (2003).
20. Minamiyama, M. *et al.* Sodium butyrate ameliorates phenotypic expression in a transgenic mouse model of spinal and bulbar muscular atrophy. *Hum. Mol. Genet.* **13**, 1183–1192 (2004).
21. Chevalier-Larsen, E.S. *et al.* Castration restores function and neurofilament alterations of aged symptomatic males in a transgenic mouse model of spinal and bulbar muscular atrophy. *J. Neurosci.* **24**, 4778–4786 (2004).
22. Ohtsu, H. *et al.* Antitumor agents. 217. Curcumin analogues as novel androgen receptor antagonists with potential as anti-prostate cancer agents. *J. Med. Chem.* **45**, 5037–5042 (2002).
23. Walcott, J.L. & Merry, D.E. Ligand promotes intranuclear inclusions in a novel cell model of spinal and bulbar muscular atrophy. *J. Biol. Chem.* **277**, 50855–50859 (2002).
24. Sopher, B.L. *et al.* Androgen receptor YAC transgenic mice recapitulate SBMA motor neuronopathy and implicate VEGF164 in the motor neuron degeneration. *Neuron* **41**, 687–699 (2004).
25. Waza, M. *et al.* 17-AAG, an Hsp90 inhibitor, ameliorates polyglutamine-mediated motor neuron degeneration. *Nat. Med.* **11**, 1088–1095 (2005).
26. Goetz, M.P., Toft, D.O., Ames, M.M. & Erlichman, C. The Hsp90 chaperone complex as a novel target for cancer therapy. *Ann. Oncol.* **14**, 1169–1176 (2003).
27. Solit, D.B. *et al.* 17-Allylamino-17-demethoxygeldanamycin induces the degradation of androgen receptor and HER-2/neu and inhibits the growth of prostate cancer xenografts. *Clin. Cancer Res.* **8**, 986–993 (2002).
28. Barent, R.L. *et al.* Analysis of FKBP51/FKBP52 chimeras and mutants for Hsp90 binding and association with progesterone receptor complexes. *Mol. Endocrinol.* **12**, 342–354 (1998).
29. Smith, D.F. *et al.* Progesterone receptor structure and function altered by geldanamycin, an hsp90-binding agent. *Mol. Cell. Biol.* **15**, 6804–6812 (1995).
30. Hostein, I., Robertson, D., DiStefano, F., Workman, P. & Clarke, P.A. Inhibition of signal transduction by the Hsp90 inhibitor 17-allylamino-17-demethoxygeldanamycin results in cytostasis and apoptosis. *Cancer Res.* **61**, 4003–4009 (2001).
31. Banerji, U. *et al.* Phase I pharmacokinetic and pharmacodynamic study of 17-allylamino, 17-demethoxygeldanamycin in patients with advanced malignancies. *J. Clin. Oncol.* **23**, 4152–4161 (2005).
32. Price, J.T. *et al.* The heat shock protein 90 inhibitor, 17-allylamino-17-demethoxygeldanamycin, enhances osteoclast formation and potentiates bone metastasis of a human breast cancer cell line. *Cancer Res.* **65**, 4929–4938 (2005).
33. Thin, T.H. *et al.* Mutations in the helix 3 region of the androgen receptor abrogate ARA70 promotion of 17beta-estradiol-induced androgen receptor transactivation. *J. Biol. Chem.* **277**, 36499–36508 (2002).
34. Wang, L. *et al.* Suppression of androgen receptor-mediated transactivation and cell growth by the glycogen synthase kinase 3 beta in prostate cells. *J. Biol. Chem.* **279**, 32444–32452 (2004).
35. Garden, G.A. *et al.* Polyglutamine-expanded ataxin-7 promotes non-cell-autonomous purkinje cell degeneration and displays proteolytic cleavage in ataxic transgenic mice. *J. Neurosci.* **22**, 4897–4905 (2002).
36. Adachi, H. *et al.* Transgenic mice with an expanded CAG repeat controlled by the human AR promoter show polyglutamine nuclear inclusions and neuronal dysfunction without neuronal cell death. *Hum. Mol. Genet.* **10**, 1039–1048 (2001).
37. Terao, S. *et al.* Age-related changes in human spinal ventral horn cells with special reference to the loss of small neurons in the intermediate zone: a quantitative analysis. *Acta Neuropathol. (Berl.)* **92**, 109–114 (1996).

ELSEVIER

Neurobiology of Disease

www.elsevier.com/locate/ynbdi
Neurobiology of Disease 25 (2007) 331–341

Dorfin-CHIP chimeric proteins potently ubiquitylate and degrade familial ALS-related mutant SOD1 proteins and reduce their cellular toxicity

Shinsuke Ishigaki,[a,b] Jun-ichi Niwa,[a] Shin-ichi Yamada,[a] Miho Takahashi,[a] Takashi Ito,[a] Jun Sone,[a] Manabu Doyu,[a] Fumihiko Urano,[b,c] and Gen Sobue[a,*]

[a]*Department of Neurology, Nagoya University Graduate School of Medicine, Nagoya 466-8500, Japan*
[b]*Program in Gene Function and Expression, University of Massachusetts Medical School, Worcester, MA 01605, USA*
[c]*Program in Molecular Medicine, University of Massachusetts Medical School, Worcester, MA 01605, USA*

Received 19 May 2006; revised 8 September 2006; accepted 22 September 2006
Available online 6 December 2006

The ubiquitin–proteasome system (UPS) is involved in the pathogenetic mechanisms of neurodegenerative disorders, including amyotrophic lateral sclerosis (ALS). Dorfin is a ubiquitin ligase (E3) that degrades mutant SOD1 proteins, which are responsible for familial ALS. Although Dorfin has potential as an anti-ALS molecule, its life in cells is short. To improve its stability and enhance its E3 activity, we developed chimeric proteins containing the substrate-binding hydrophobic portion of Dorfin and the U-box domain of the carboxyl terminus of Hsc70-interacting protein (CHIP), which has strong E3 activity through the U-box domain. All the Dorfin-CHIP chimeric proteins were more stable in cells than was wild-type Dorfin ($Dorfin^{WT}$). One of the Dorfin-CHIP chimeric proteins, $Dorfin\text{-}CHIP^{L}$, ubiquitylated mutant SOD1 more effectively than did $Dorfin^{WT}$ and CHIP *in vivo*, and degraded mutant SOD1 protein more rapidly than $Dorfin^{WT}$ does. Furthermore, $Dorfin\text{-}CHIP^{L}$ rescued neuronal cells from mutant SOD1-associated toxicity and reduced the aggresome formation induced by mutant SOD1 more effectively than did $Dorfin^{WT}$.

Keywords: Dorfin; ALS; SOD1; CHIP; Neurodegeneration; Ubiquitin–proteasome system

Amyotrophic lateral sclerosis (ALS), one of the most common neurodegenerative disorders, is characterized by selective motor neuron degeneration in the spinal cord, brainstem, and cortex. About 10% of ALS cases are familial; of these, 10%–20% are caused by Cu/Zn superoxide dismutase (SOD1) gene mutations (Rosen et al., 1993; Cudkowicz et al., 1997). However, the precise mechanism that causes motor neuron death in ALS is still unknown, although many have been proposed: oxidative toxicity, glutamate receptor abnormality, ubiquitin proteasome dysfunction, inflammatory and cytokine activation, neurotrophic factor deficiency, mitochondrial damage, cytoskeletal abnormalities, and activation of the apoptosis pathway (Julien, 2001; Rowland and Shneider, 2001).

Misfolded protein accumulation, one probable cause of neurodegenerative disorders, including ALS, can cause the deterioration of various cellular functions, leading to neuronal cell death (Julien, 2001; Ciechanover and Brundin, 2003). Recent findings indicate that the ubiquitin–proteasome system (UPS), a cellular function that recognizes and catalyzes misfolded or impaired cellular proteins (Jungmann et al., 1993; Lee et al., 1996; Bercovich et al., 1997), is involved in the pathogenesis of various neurodegenerative diseases, among them ALS, Parkinson's disease (PD), Alzheimer's disease, polyglutamine disease, and prion disease (Alves-Rodrigues et al., 1998; Sherman and Goldberg, 2001; Ciechanover and Brundin, 2003). The ubiquitin ligase (E3), a key molecule for the UPS, can specifically recognize misfolded substrates and convey them to proteasomal degradation (Scheffner et al., 1995; Glickman and Ciechanover, 2002; Tanaka et al., 2004).

Dorfin, an E3 protein, contains an in-between-ring-finger (RING-IBR) domain at its N-terminus. The C-terminus of Dorfin can recognize mutant SOD1 proteins, which cause familial ALS (Niwa et al., 2001; Ishigaki et al., 2002b; Niwa et al., 2002). In cultured cells, Dorfin colocalized with aggresomes and ubiquitin-positive inclusions, which are pathological hallmarks of neurodegenerative diseases (Hishikawa et al., 2003; Ito et al., 2003). Dorfin also interacted with VCP/p97 in ubiquitin-positive inclusions in

Abbreviations: ALS, amyotrophic lateral sclerosis; CFTR, cystic fibrosis transmembrane conductance regulator; CHIP, carboxyl terminus of Hsc70-interacting protein; DMEM, Dulbecco's modified Eagle's medium; E3, ubiquitin ligase; FCS, fetal calf serum; IP, immunoprecipitation; LB, Lewy body; PD, Parkinson's disease; RING-IBR, in-between-ring-finger; SCF, Skp1-Cullin-F box complex; SDS-PAGE, sodium dodecyl sulfate-polyacrylamide gel electrophoresis; SOD1, Cu/Zn super oxide dismutase; UPS, ubiquitin–proteasome system.

* Corresponding author. Fax: +81 52 744 2384.
E-mail address: sobueg@med.nagoya-u.ac.jp (G. Sobue).
Available online on ScienceDirect (www.sciencedirect.com).

0969-9961/$ - see front matter © 2006 Elsevier Inc. All rights reserved.
doi:10.1016/j.nbd.2006.09.017

ALS and PD (Ishigaki et al., 2004). Moreover, formation of this complex was found to be necessary for the E3 activity of Dorfin against mutant SOD1. These findings suggest that Dorfin is involved in the quality-control system for the abnormal proteins that accumulate in the affected neurons in neurodegenerative disorders.

Dorfin degrades mutant SOD1s and attenuates mutant SOD1-associated toxicity in cultured cells (Niwa et al., 2002). However, in Dorfin/mutant SOD1 double transgenic mice, we found only a modest beneficial effect on mutant SOD1-induced survival and motor dysfunction (unpublished data). These findings, combined with the short half-life of Dorfin protein, led us to hypothesize that the limiting effect of the Dorfin transgene may be a consequence of autodegradation of Dorfin, since Dorfin can execute autoubiquitilation *in vivo* (Niwa et al., 2001).

Carboxyl terminus of Hsc70-interacting protein (CHIP) is also an E3 protein; it has a TPR domain in the N terminus and a U-box domain in the C terminus. The U-box domain of CHIP is responsible for its strong E3 activity, whereas the TPR domain recruits heat shock proteins harboring misfolded client proteins such as cystic fibrosis transmembrane conductance regulator (CFTR), denatured luciferase, and tau (Meacham et al., 2001; Murata et al., 2001, 2003; Hatakeyama et al., 2004; Shimura et al., 2004).

To prolong the protein lifetime of Dorfin and thereby obtain more potent ubiquitylation and degradation activity against mutant SOD1s than is provided by Dorfin or CHIP alone, we generated chimeric proteins containing the substrate-binding domain of Dorfin and the UPR domain of CHIP substitute for RING/IBR of Dorfin. We developed 12 candidate constructs that encode Dorfin-CHIP chimeric proteins and analyzed them for their E3 activities and degradation abilities against mutant SOD1 protein in cultured cells.

Experimental procedures

Plasmids and antibodies

We designed constructs expressing Dorfin-CHIP chimeric protein. In these constructs, different-length fragments of the C-terminus portion of Dorfin, including the hydrophobic substrate-binding domain (amino acids 333–838, 333–700, and 333–454) and the C-terminus UPR domain of CHIP with amino acids 128–303 or without amino acids 201–303, a charged region was fused in various combinations as shown in Fig. 2C. Briefly, Dorfin-CHIP$^{A, B, C, G, H,}$ and ^{I} had the C-terminus portion of Dorfin in their N-terminus and the U-box of CHIP in their C-terminus; Dorfin-CHIP$^{D, E, F, J, K}$, and ^{L} had the U-box of CHIP in their N-terminus and the C-terminus portion of Dorfin in their C-terminus.

We prepared a pCMV2/FLAG-Dorfin-CHIP chimeric vector (Dorfin-CHIP) by polymerase chain reaction (PCR) using the appropriate design of PCR primers with restriction sites (*Cla*I, *Kpn*I, and *XBa*I or *Eco*RI, *Cla*I, and *Kpn*I). The PCR products were digested and inserted into the *Cla*I–*Kpn*I site in pCMV2 vector (Sigma, St. Louis, MO). These vectors have been described previously: pFLAG-Dorfin^{WT} (Dorfin^{WT}), FLAG-Dorfin$^{C132S/C135S}$ (Dorfin$^{C132S/C135S}$), pFLAG-CHIP (CHIP), pFLAG-Mock (Mock), pcDNA3.1/Myc-SOD1^{WT} (SOD1^{WT}), pcDNA3.1/Myc-SOD1^{G93A} (SOD1^{G93A}), pcDNA3.1/Myc-SOD1^{G85R} (SOD1^{G85R}), pcDNA3.1/Myc-SOD1^{H46R} (SOD1^{H46R}), pcDNA3.1/Myc-SOD1^{G37R} (SOD1^{G37R}), pEGFP/SOD1^{WT} (SOD1^{WT}-GFP), and pEGFP/SOD1^{G85R} (SOD1^{G85R}-GFP) (Ishigaki et al., 2004). We used monoclonal anti-FLAG antibody (M2; Sigma), monoclonal anti-Myc antibody (9E10; Santa Cruz Biotechnology, Santa Cruz, CA), monoclonal anti-HA antibody (12CA5; Roche, Basel, Switzerland), and polyclonal anti-SOD1 (SOD-100; Stressgen, San Diego, CA).

Cell culture and transfection

We grew HEK293 cells and neuro2a (N2a) cells in Dulbecco's modified Eagle's medium (DMEM) containing 10% fetal calf serum (FCS), 5 U/ml penicillin, and 50 μg/ml streptomycin. At subconfluence, we transfected these cells with the indicated plasmids, using Effectene reagent (Qiagen, Valencia, CA) for HEK293 cells and Lipofectamine 2000 (Invitrogen, Carlsbad, CA) for N2a cells. After overnight posttransfection, we treated the cells with 1 μM MG132 (Z-Leu-Leu-Leu-al; Sigma) for 16 h to inhibit cellular proteasome activity. We analyzed the cells 24–48 h after transfection. To differentiate N2a cells, cells were treated for 48 h with 15 μM of retinoic acid in 2% serum medium.

Immunological analysis

At 24–48 h after transfection, we lysed cells (4×10^5 in 6-cm dishes) with 500 μl of lysis buffer consisting of 50 mM Tris–HCl, 150 mM NaCl, 1% Nonidet P-40, and 1 mM ethylenediaminetetraacetic acid (EDTA), as well as a protease inhibitor cocktail (Complete Mini, Roche). The lysate was then centrifuged at $10{,}000\times g$ for 10 min at 4°C to remove debris. We used a 10% volume of the supernatants as the lysate for SDS-PAGE. When immunoprecipitated, the supernatants were precleared with protein A/G agarose (Santa-Cruz). A specific antibody, either anti-FLAG (M2) or anti-Myc (9E10), was then added. We incubated the immune complexes, first at 4°C with rotation and with protein A/G agarose (Roche) for 3 h, after which they were collected by centrifugation and washed four times with the lysis buffer. For protein analysis, immune complexes were dissociated by heating in SDS-PAGE sample buffer and loaded onto SDS-PAGE. We separated the samples by SDS-PAGE (15% gel or 5%–20% gradient gel) and transferred them onto polyvinylidene difluoride membranes. We then immunoblotted samples with specific antibodies.

Immunohistochemistry

We fixed differentiated N2a cells grown in plastic dishes in 4% paraformaldehyde in PBS for 15 min. The cells were then blocked for 30 min with 5% (vol/vol) normal goat serum in PBS, incubated overnight at 4°C with anti-FLAG antibody (M2), washed with PBS, and incubated for 30 min with Alexa 496 nm anti-mouse antibodies (Molecular Probes, Eugene, OR). We mounted the cells on slides and obtained images using a fluorescence microscope (IX71; Olympus, Tokyo, Japan) equipped with a cooled charge-coupled device camera (DP70; Olympus). Photographs were taken using DP Controller software (Olympus).

Analysis of protein stability

We assayed the stability of proteins by pulse-chase analysis using [^{35}S] followed by immunoprecipitation. Metabolic labeling was performed as described previously (Yoshida et al., 2003). Briefly, in the pulse-chase analysis of Dorfin proteins, HEK293 cells in 6-cm dishes were transiently transfected with 1 μg of

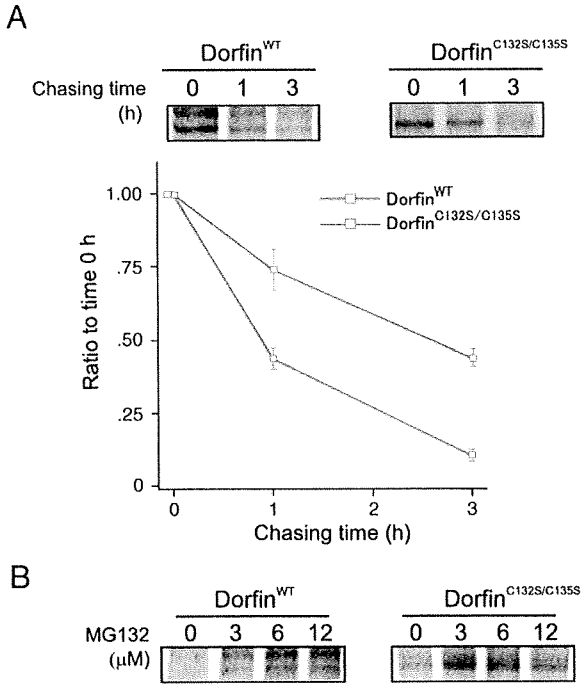

Fig. 1. Pulse-chase analysis of Dorfin^{WT} and Dorfin$^{C132S/C135S}$. (A) Dorfin^{WT} or Dorfin$^{C132S/C135S}$ was overexpressed in HEK293 cells. After overnight incubation, [^{35}S]-labeled Met/Cys pulse-chase analysis was performed. Cells were harvested and analyzed at 0, 1, or 3 h after labeling and immunoprecipitation by anti-FLAG antibody (upper panels). To determine serial changes in the amount of Dorfin^{WT} or Dorfin$^{C132S/C135S}$, four independent experiments were performed and the amounts of Dorfin^{WT} and Dorfin$^{C132S/C135S}$ were plotted. The differences between the amounts of Dorfin^{WT} and Dorfin$^{C132S/C135S}$ were significant at 1 h ($p<0.01$) and 3 h after labeling ($p<0.001$) (lower panels). Values are the means±SE, $n=4$. Statistics were done using an unpaired t-test. (B) Cells overexpressing Dorfin^{WT} or Dorfin$^{C132S/C135S}$ were treated with different concentrations of MG132 for 3 h after labeling.

FLAG-Dorfin^{WT} or FLAG-Dorfin$^{C132S/C135S}$. In pulse-chase experiments using SOD1^{G85R}, N2a cells in 6-cm dishes were transiently transfected with 1 μg of SOD1^{G85R}-Myc or SOD1^{G93A}-Myc and FLAG-Mock, FLAG-Dorfin, or FLAG-Dorfin-CHIP^{L}. FLAG-Mock was used as a negative control. After starving the cells for 60 min in methionine- and cysteine-free DMEM with 10% FCS, we labeled them for 60 min with 150 μCi/ml of Pro-Mix L-[^{35}S] *in vitro* cell-labeling mix (Amersham Biosciences). Cells were chased for different lengths of time at 37°C. In experiments with proteasomal inhibition, we added different amounts of MG132 in medium during the chase period. We performed immunoprecipitation using protein A/G agarose, mouse monoclonal anti-FLAG (M2), and anti-Myc (9E10). The intensity of the bands was quantified by ImageGauge software (Fuji Film, Tokyo, Japan).

MTS assay

We transfected N2a cells (5000 cells per well) in 96-well collagen-coated plates with 0.15 μg of SOD1^{G85R}-GFP and 0.05 μg of Dorfin, CHIP, Dorfin-CHIP^{L}, or pCMV2 vector (Mock) using Effecten reagent (Qiagen). Then we performed 3-(4,5-dimethylthiazol-2-yl)-5-(3-carboxymethoxyphenyl)-2-(4-sulfophenyl)-2*H*-tetrazolium inner salt (MTS) assays using Cell Titer 96 (Promega) at 48 h after incubation. This procedure has previously been described (Ishigaki et al., 2002a).

Aggregation assay

We transfected N2a cells in 6-cm dishes with 1.0 μg of SOD1^{G85R}-GFP and 1.0 μg of FLAG-Mock, FLAG-Dorfin, FLAG-CHIP, or FLAG-Dorfin-CHIP^{L}. After overnight incubation, we changed the medium to 2% FCS containing medium with 15 μM retinoic acid (RA) for differentiation. In the MG132 (+) group, 1 μM of MG132 was added after 24 h of differentiation stimuli. After 48 h of differentiation stimuli, we examined the cells in their living condition by fluorescence microscopy. The transfection ratio was equivalent (75%) among all groups. Visually observable macro aggregation-harboring cells were counted as "aggregation positive" cells (Fig. 7C). All cells were counted in fields selected at random from the four different quadrants of the culture dish. Counting was done by an investigator who was blind to the experimental condition.

Results

Dorfin degradation by the UPS in vivo

We analyzed the degradation speed of FLAG-Dorfin by the pulse-chase method using [^{35}S] labeling, finding that more than half of wild-type Dorfin (Dorfin^{WT}) was degraded within 1 h (Fig. 1A). This degradation was dose-dependently inhibited by MG132, a proteasome inhibitor (Fig. 1B). On the other hand, the RING mutant form of Dorfin (Dorfin$^{C132S/C135S}$), which lacks E3 activity (Ishigaki et al., 2004), degraded significantly more slowly than did Dorfin^{WT} (Fig. 1A and Table 1). As shown in Fig. 1A, Dorfin^{WT} showed two bands, whereas Dorfin$^{C132S/C135S}$ had a single band. This was also seen in our previous study (Ishigaki et al., 2004) and may represent posttranslational modification.

Construction of Dorfin-CHIP chimeric proteins

It is known that the C-terminus portion of Dorfin can bind to substrates such as mutant SOD1 proteins or Synphilin-1 (Niwa et al., 2002; Ito et al., 2003). We attempted to identify the domain of Dorfin that interacts with substrates. Although there was no obvious known motif in the C-terminus of Dorfin (amino acids 333–838), its first quarter contained rich hydrophobic amino acids (amino acids 333–454) (Fig. 2A). Immunoprecipitation analysis revealed that the hydrophobic region of Dorfin (amino acids 333–454) was able to bind to SOD1^{G85R}, indicating that this hydrophobic region is responsible for recruiting mutant SOD1 in Dorfin protein (Fig. 2B).

To establish more effective and more stable E3 ubiquitin ligase molecules that can recognize and degrade mutant SOD1s, we

Table 1
Serial changes in the amounts of Dorfin^{WT}, Dorfin$^{C132S/C135S}$, and Dorfin-CHIP^{L}

	0 h (%)	1 h (%)	3 h (%)
Dorfin^{WT}	100	43.7±7.0	10.3±4.4
Dorfin$^{C132S/C135S}$	100	73.9±13.8	43.7±1.9
Dorfin-CHIP^{L}	100	89.0±5.7	47.5±5.3

Values are the mean and SD of four independent experiments.

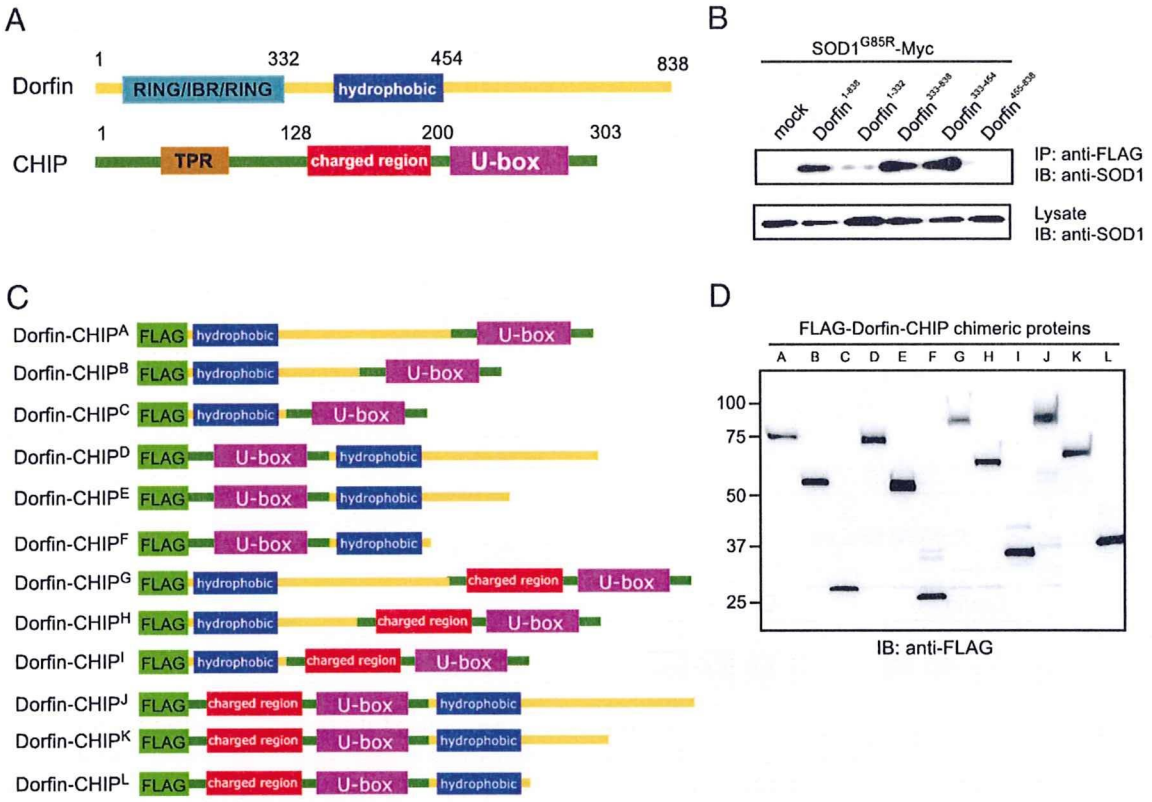

Fig. 2. Construction of Dorfin-CHIP chimeric proteins. (A) Dorfin has a RING/IBR domain in its N-terminus and a substrate-binding portion in the C-terminus. CHIP contains a TPR domain that binds to heat-shock proteins at the N-terminus; its C-terminal U-box domain has strong E3 ubiquitin ligase activity. (B) SOD1^{G85R}-Myc and FLAG-Dorfin derivatives were overexpressed in HEK 293 cells. Cell lysates were immunoprecipitated with anti-myc antibody. Immunoblotting showed that FLAG-Dorfin derivatives containing Dorfin$^{333–454}$ bound to SOD1^{G85R}-Myc, indicating that the hydrophobic region of Dorfin (Dorfin$^{333–454}$) is essential for interaction with mutant SOD1 *in vivo*. (C) Scheme of engineered Dorfin-CHIP chimeric proteins. Three different lengths of C-terminal Dorfin containing the hydrophobic region of Dorfin (Dorfin$^{333–454}$) and the U-box domain of CHIP with or without the charged region were fused. (D) Dorfin-CHIP chimeric proteins were overexpressed in HEK293 cells. Harvested cells were lysed and analyzed by immunoblotting using anti-FLAG antibody.

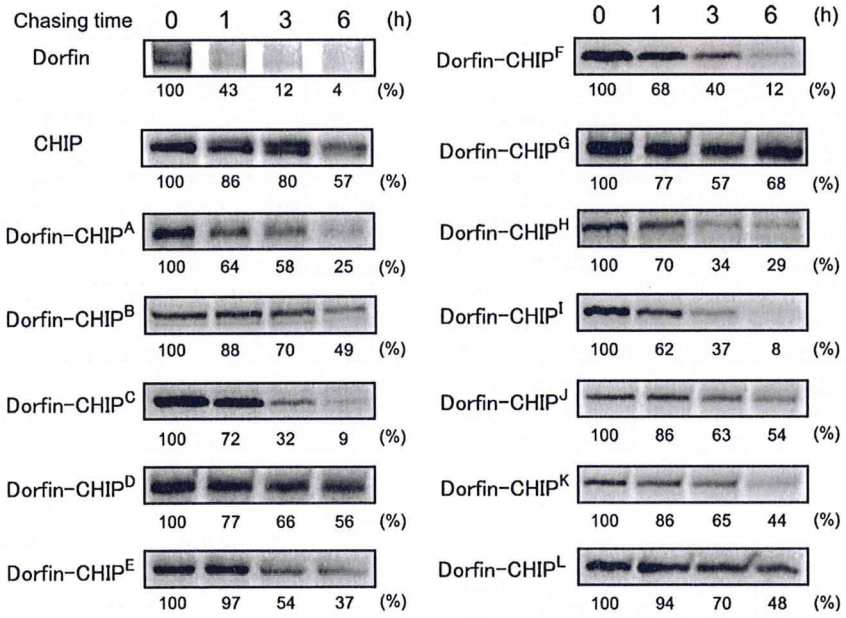

Fig. 3. The stability of Dorfin-CHIP chimeric proteins. Pulse-chase analysis using [^{35}S]-Met/Cys was performed. Dorfin, CHIP, and all the Dorfin-CHIP chimeric proteins were overexpressed in HEK293 cells and labeled with [^{35}S]-Met/Cys. Immunoprecipitation using anti-FLAG antibody and SOD-PAGE analysis revealed the degradation speed of FLAG-Dorfin-CHIP chimeric proteins. The amount of each Dorfin-CHIP chimeric protein was measured by quantifying the band using ImageGauge software.

designed Dorfin-CHIP chimeric proteins containing both the hydrophobic substrate-binding domain of Dorfin and the U-box domain of CHIP, which has strong E3 activity (Fig. 2C). We verified that all of the 12 candidate chimeric proteins were expressed in HEK293 cells (Fig. 2D).

Expression of Dorfin-CHIP chimeric proteins in cells

The half lives of all the Dorfin-CHIP chimeric proteins were more than 1 h. In some of these proteins, such as Dorfin-CHIP$^{D, G, J}$, and ^{L}, moderate amounts of protein still remained at 6 h after labeling, indicating that they were degraded much more slowly than was Dorfin^{WT} (Fig. 3). Repetitive experiments using Dorfin-CHIP^{L} yielded a significant difference between the amount of Dorfin^{WT} and Dorfin-CHIP^{L} at 1 h and 3 h (Table 1).

E3 activity of Dorfin-CHIP chimeric proteins against mutant SOD1

Immunoprecipitation analysis demonstrated that Dorfin and CHIP bound to mutant SOD1^{G85R} in equivalent amounts and that all of the Dorfin-CHIP chimeric proteins interacted with mutant SOD1^{G85R} *in vivo*. Dorfin-CHIP$^{A, D, E, F, J, K}$, and ^{L} bound to the same or greater amounts of SOD1^{G85R} than did Dorfin, whereas Dorfin-CHIP$^{B, C, G, H}$, and ^{I} did not (Fig. 4A, upper panel). None of the Dorfin-CHIP chimeric proteins bound to SOD1^{WT} *in vivo*

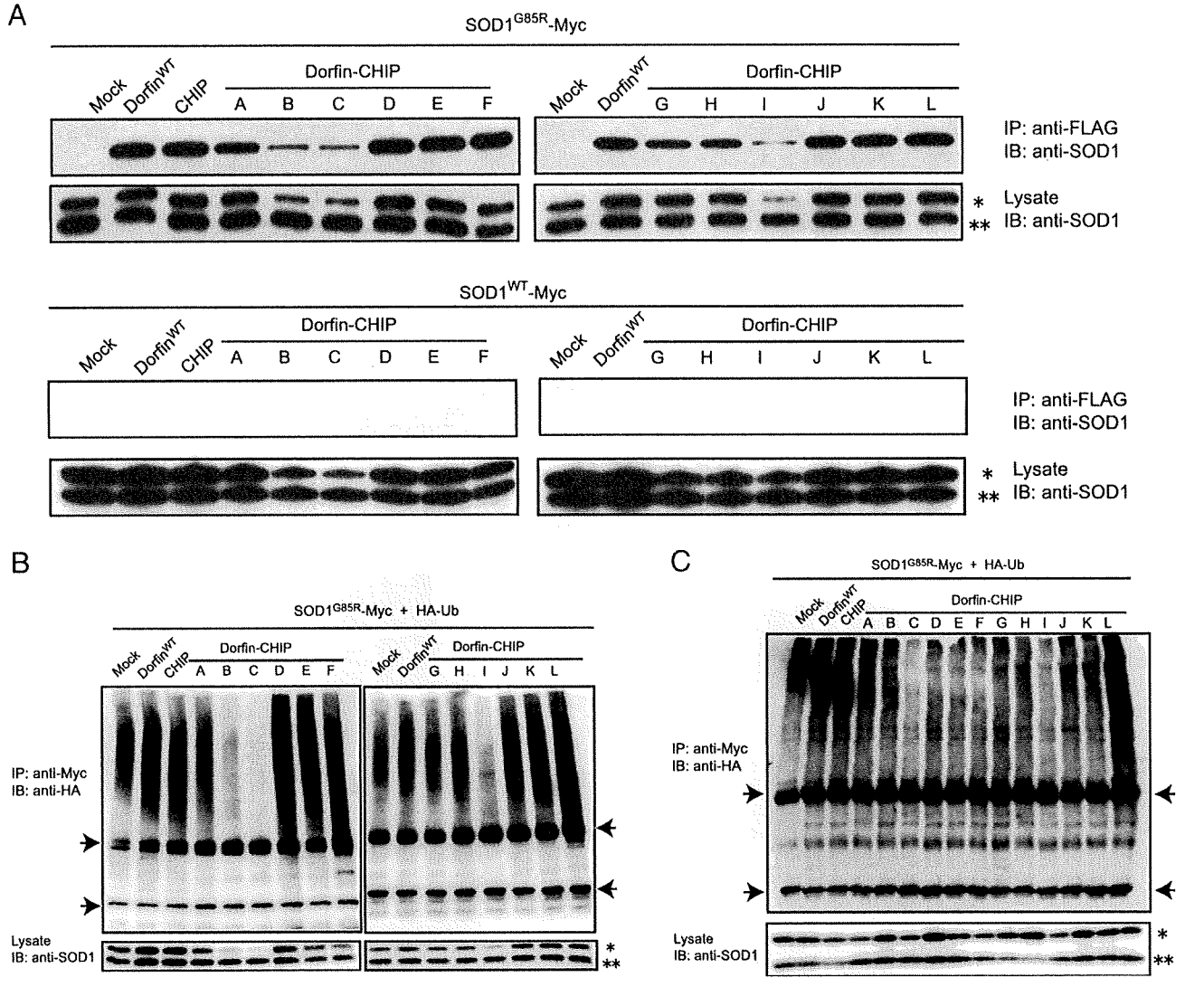

Fig. 4. The E3 activity of Dorfin-CHIP chimeric proteins on mutant SOD1 *in vivo*. (A) *In vivo* binding assay with both wild-type and mutant SOD1s. SOD1^{G85R}- or SOD1^{WT}-Myc and FLAG derivatives of Dorfin-CHIP chimeric proteins were coexpressed in HEK293 cells. Immunoprecipitation was done using anti-Myc antibody. Immunoblotting with anti-FLAG antibody revealed that all the Dorfin-CHIP chimeric proteins bound *in vivo* to SOD1^{G85R}-Myc but not to SOD1^{WT}-Myc. Single and double asterisks indicate overexpressed human SOD1s and mouse endogenous SOD1, respectively. (B) *In vivo* ubiquitylation assay in HEK293 cells. SOD1^{G85R}-Myc, HA-Ub, and FLAG derivatives of Dorfin-CHIP chimeric proteins were coexpressed in HEK293 cells. Immunoblotting with anti-HA antibody demonstrated the ubiquitylation level of SOD1^{G85R}-Myc by FLAG derivatives of Dorfin-CHIP chimeric proteins *in vivo*. Arrows indicate IgG light and heavy chains. Single and double asterisks indicate overexpressed SOD1 and mouse endogenous SOD1, respectively. (C) *In vivo* ubiquitylation assay in N2a cells. SOD1^{G85R}-Myc, HA-Ub, and FLAG derivatives of Dorfin-CHIP chimeric proteins were coexpressed in N2a cells. Arrows indicate IgG light and heavy chains. Single and double asterisks indicate overexpressed human SOD1s and mouse endogenous SOD1, respectively.

(Fig. 4A, lower panel). Some Dorfin-CHIP chimeric proteins, such as Dorfin-CHIP$^{B, C}$, and ^{I}, had lower amounts of both SOD1^{WT} and SOD1^{G85R} in the lysates. We performed quantitative RT-PCR using specific primers for SOD1-Myc, finding that coexpression of Dorfin-CHIP$^{B, C}$ or ^{I} suppressed the mRNA expression of overexpressed SOD1 gene (Supplementary Fig. 1). Considering the possibility that these Dorfin-CHIP chimeric proteins might have unpredicted toxicity for cells by affecting gene transcription via unknown mechanisms, we excluded them from further analysis. Other Dorfin-CHIP proteins did not affect SOD1-Myc gene expression, which validated the comparison among IPs and ubiquitylated mutant SOD1 in Figs. 4A–C.

To assess the effectiveness of the E3 activity of Dorfin-CHIP chimeric proteins, we did an *in-vivo* ubiquitylation analysis by coexpression of SOD1^{G85R}-Myc, HA-Ub, and Dorfin-CHIP chimeric proteins in HEK293 cells. We found that Dorfin and CHIP enhanced the ubiquitylation of SOD1^{G85R} protein and that the ubiquitylation levels of these two E3 ligases were almost equivalent. Moreover, Dorfin-CHIP$^{D, E, F, J, K}$, and ^{L} ubiquitylated SOD1^{G85R} more effectively than did Dorfin or CHIP (Fig. 4B).

Performing the same *in-vivo* ubiquitylation assay using N2a cells, we observed that the levels of ubiquitylation of SOD1^{G85R} by Dorfin and CHIP were equivalent, as they were in HEK293 cells. Among Dorfin-CHIP chimeric proteins, only Dorfin-CHIP^{L}

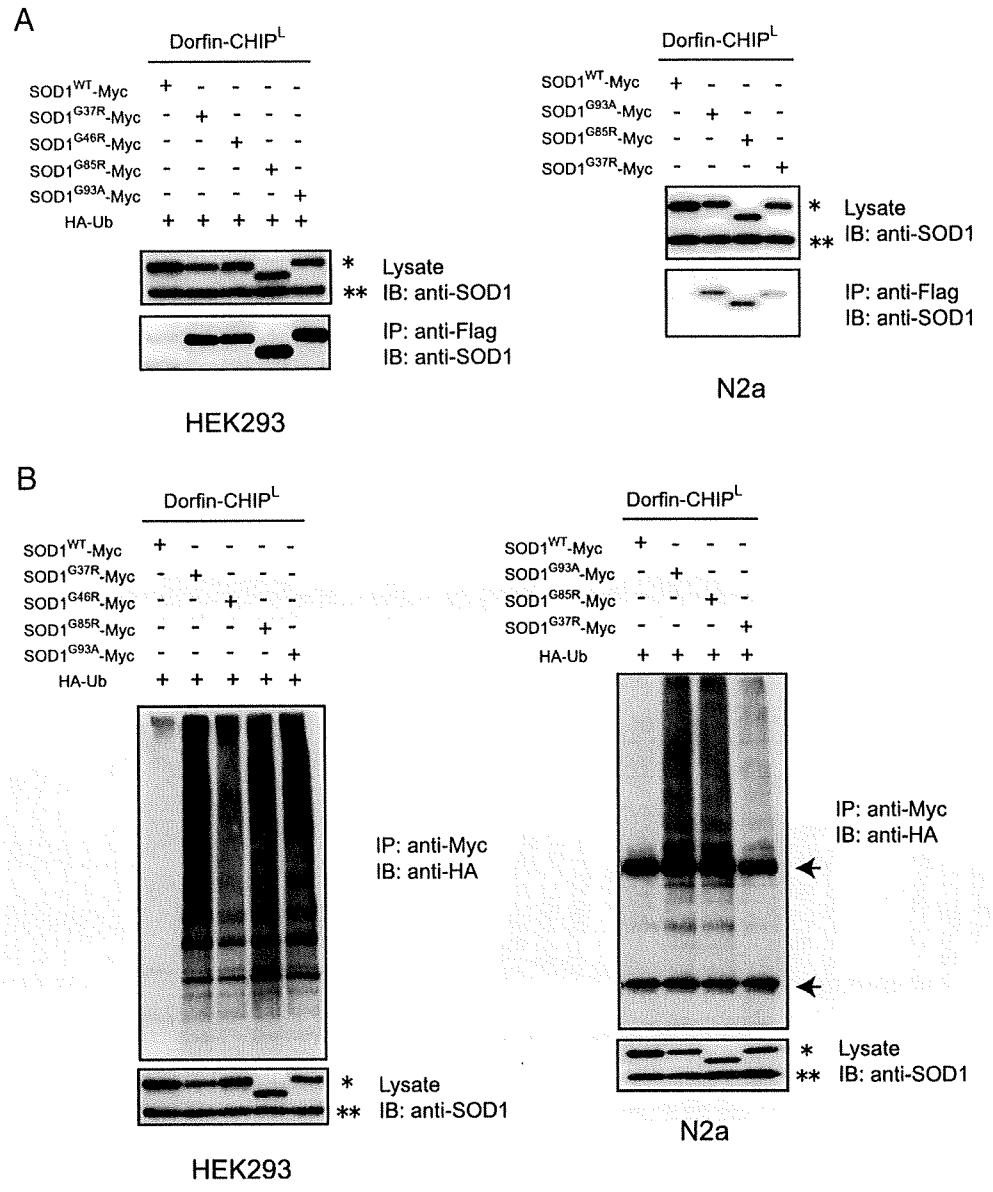

Fig. 5. Dorfin-CHIP^{L} specifically ubiquitylates mutant SOD1s *in vivo*. (A) *In vivo* binding assay with various mutant SOD1s. SOD1^{WT}-Myc, SOD1^{G93A}-Myc, SOD1^{G85R}-Myc, SOD1^{H46R}-Myc or SOD1^{G37R}-Myc, and FLAG-Dorfin-CHIP^{L} were coexpressed in HEK293 (left) and N2a cells (right). Immunoprecipitation was done using anti-Myc antibody. Immunoblotting with anti-FLAG antibody showed that both chimeric proteins specifically bound to mutant SOD1s *in vivo*. Single and double asterisks indicate overexpressed SOD1 and mouse endogenous SOD1, respectively. (B) *In vivo* ubiquitylation assay. SOD1^{WT}-Myc, SOD1^{G93A}-Myc, SOD1^{G85R}-Myc, SOD1^{H46R}-Myc or SOD1^{G37R}-Myc, as well as FLAG-Dorfin-CHIP^{L} and HA-Ub, was coexpressed in HEK293 (left) and N2a cells (right). Immunoblotting with anti-HA antibody showed the specific ubiquitylation of mutant SOD1-Myc by FLAG-Dorfin-CHIP^{L} *in vivo*. Arrows indicate IgG light and heavy chains. Single and double asterisks indicate overexpressed human SOD1s and mouse endogenous SOD1, respectively.

ubiquitylated SOD1^{G85R} more effectively than did Dorfin or CHIP, while Dorfin-CHIP$^{D, E, F, J}$, and ^{K} did not (Fig. 4C). Thus, Dorfin-CHIP^{L} was the most potent candidate of the chimeric proteins.

Ubiquitylation of mutant SOD1 by Dorfin-CHIP^{L}

Dorfin specifically ubiquitylated mutant SOD1 proteins, but not SOD1^{WT} protein (Niwa et al., 2002; Ishigaki et al., 2004). Similarly, Dorfin-CHIP^{L} interacted with SOD1^{G93A}, SOD1^{G85R}, SOD1^{H46R}, and SOD1^{G37R}, but not SOD1^{WT}, in HEK293 cells. This was confirmed in N2a cells (Fig. 5A). In both HEK293 and N2a cells, Dorfin-CHIP^{L} also ubiquitylated mutant SOD1 proteins but not SOD1^{WT} (Fig. 5B).

Degradation of mutant SOD1 by Dorfin-CHIP chimeric proteins

To assess the degradation activity of Dorfin-CHIP^{L} against mutant SOD1s, we performed the pulse-chase analysis on N2a

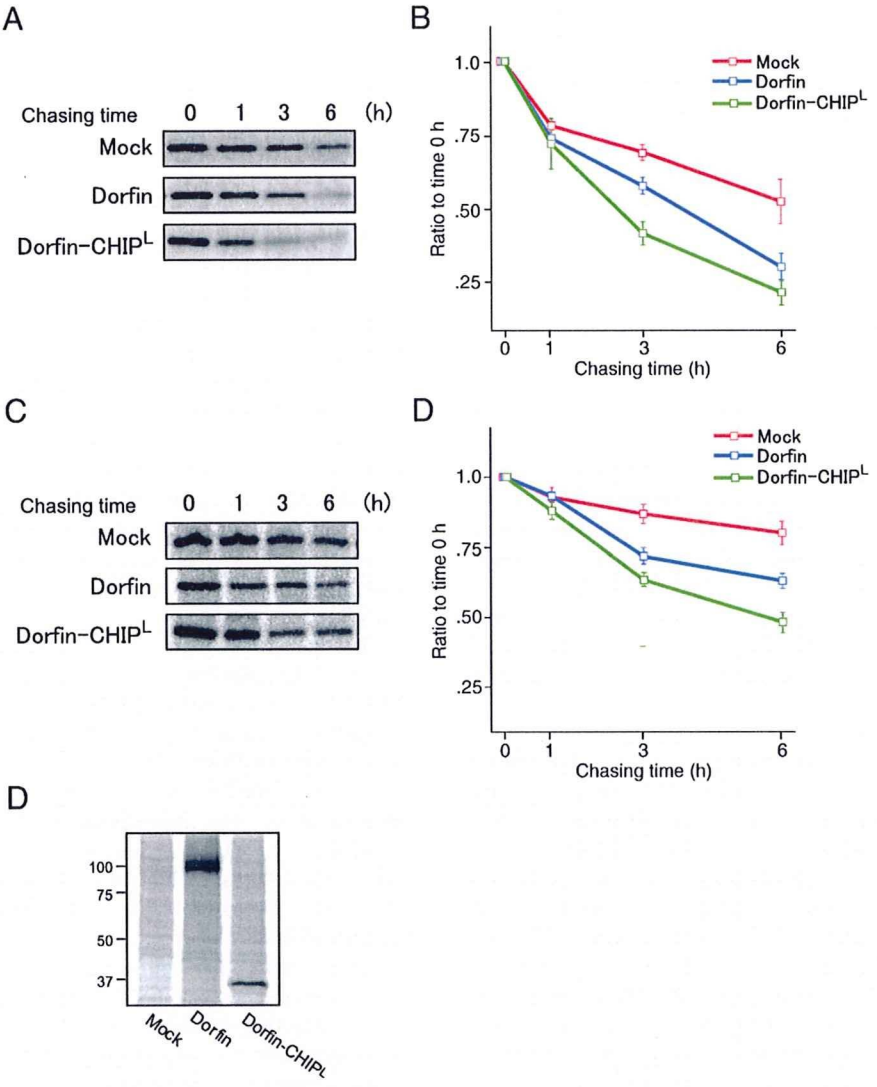

Fig. 6. Degradation of mutant SOD1 proteins with Dorfin-CHIP^{L}. (A) Pulse-chase analysis of SOD1^{G85R} with Dorfin-CHIP^{L}. N2a cells were coexpressed with SOD1^{G85R}-Myc and Mock, Dorfin, and Dorfin-CHIP^{L}. Pulse-chase experiments using [^{35}S]-Met/Cys were done. Immunoprecipitation using anti-Myc antibody and SOD-PAGE analysis revealed the degradation speed of SOD1^{G85R}-Myc. (B) Serial changes in the amount of SOD1^{G85R} coexpressed with Mock, Dorfin, or Dorfin-CHIP^{L}. Four independent experiments were performed and the amounts of SOD1^{G85R} were plotted. There were significant differences between Mock and Dorfin ($p<0.005$), Mock and Dorfin-CHIP^{L} ($p<0.005$), and Dorfin and Dorfin-CHIP^{L} ($p<0.05$) at 3 h, as well as between Mock and Dorfin ($p<0.05$), and Mock and Dorfin-CHIP^{L} ($p<0.05$) at 6 h after labeling. Values are the means±SE, $n=4$. Statistical analysis was done by one-way ANOVA. (C) Pulse-chase analysis of SOD1^{G93A} with Dorfin-CHIP^{L}. N2a cells were coexpressed with SOD1^{G93A}-Myc and Mock, Dorfin, and Dorfin-CHIP^{L} as in panel A. (D) Serial changes in the amount of SOD1^{G93A} coexpressed with Mock, Dorfin, or Dorfin-CHIP^{L}. Four independent experiments were performed and the amounts of SOD1^{G93A} were plotted. There were significant differences between Mock and Dorfin ($p<0.05$) and Mock and Dorfin-CHIP^{L} ($p<0.01$) at 3 h, as well as between Mock and Dorfin ($p<0.05$), Mock and Dorfin-CHIP^{L} ($p<0.01$), and Dorfin and Dorfin-CHIP^{L} ($p<0.05$) at 6 h after labeling. Values are the means±SE, $n=4$. Statistics were done by one-way ANOVA. (E) The equivalent protein expression levels of Dorfin and Dorfin-CHIP^{L}. Half of the volume of samples used in the pulse-chase analysis of panel C at 0 h was used for immunoprecipitation using anti-Flag M2 antibody. The following SOD-PAGE analysis revealed the amounts of Dorfin and Dorfin-CHIP^{L} in the experiment shown in panel C.

cells, using [^{35}S] labeled Met/Cys. The protein levels of SOD1^{G85R} and SOD1^{G93A} declined more rapidly with Dorfin coexpression. Dorfin-CHIP^{L} remarkably declined in both SOD1^{G85R} and SOD1^{G93A} (Figs. 6A, C). Dorfin and Dorfin-CHIP^{L} had similar expression levels at 0 h of this experiment (Fig. 6E). As compared to Mock, Dorfin showed significant declines of both SOD1^{G85R} at 3 h ($p<0.001$) and 6 h ($p<0.05$) after labeling, as shown in a previous study (Niwa et al., 2002). Dorfin-CHIP^{L} also significantly accelerated the decline of SOD1^{G85R} at 3 h ($p<0.001$) and 6 h ($p<0.05$) after labeling again as compared to Mock. At 3 h after labeling, a significant difference between Dorfin-CHIP^{L} and Dorfin was present with respect to SOD1^{G85R} degradation ($p<0.05$). As compared to Dorfin, Dorfin-CHIP^{L} also tended toward accelerated SOD1^{G85R} degradation at 6 h after labeling (Fig. 6B). Similarly, Dorfin showed significant declines of SOD1^{G93A} at 3 h ($p<0.05$) and 6 h ($p<0.05$) after labeling, and Dorfin-CHIP^{L} significantly accelerated the declines of SOD1^{G93A} at 3 h ($p<0.01$) and 6 h ($p<0.01$) after labeling as compared to Mock. A significant difference between Dorfin-CHIP^{L} and Dorfin was present at 6 h in SOD1^{G93A} degradation ($p<0.05$) (Fig. 6D).

Attenuation of the toxicity of mutant SOD1 and decrease in the formation of visible aggregations of mutant SOD1 in cultured neuronal culture cells

The ability of Dorfin-CHIP chimeric proteins to attenuate mutant SOD1-related toxicity was analyzed by MTS assay using N2a cells. The expression of SOD1^{G85R}, as compared to that of SOD1^{WT}, decreased the viability of cells. Overexpression of Dorfin reversed the toxic effect of SOD1^{G85R}, whereas overexpression of CHIP did not. Dorfin-CHIP^{L} had a significantly greater rescue effect on SOD1^{G85R}-related cell toxicity than did Dorfin (Fig. 7A). We also measured the cell viability of N2a cells overexpressing Mock, Dorfin, and Dorfin-CHIP^{L} with various amounts of constructs, and found no difference in toxicity among them (Supplementary Fig. 2).

A structure that Johnston et al. (1998) called aggresome is formed when the capacity of a cell to degrade misfolded proteins is exceeded. The accumulation of mutant SOD1 induces visible macroaggregation, which is considered to be 'aggresome' in N2a cells. We examined the subcellular localizations of Dorfin, CHIP, and Dorfin-CHIP^{L} by immunostaining N2a cells expressing SOD1^{G85R}-GFP. Dorfin was localized in aggresomes with substrate proteins, as in our previous studies. Dorfin-CHIP^{L} was also seen in aggresomes, whereas the staining of CHIP was diffusely observed in the cytosol (Fig. 7B). We counted these visible aggregations with or without MG132 treatment. Dorfin decreased the number of aggregation-containing cells, as has been reported (Niwa et al., 2002), but Dorfin-CHIP^{L} did so more effectively. These effects were inhibited by the treatment of MG132 (Fig. 7C).

Discussion

E3 proteins can specifically recognize and degrade accumulating aberrant proteins, which are deeply involved in the pathogenesis of neurodegenerative disorders, including ALS (Alves-Rodrigues et al., 1998; Sherman and Goldberg, 2001; Ciechanover and Brundin, 2003). For this reason, E3 proteins are candidate molecules for use in developing therapeutic technology for neurodegenerative diseases. Dorfin is the first E3 molecule that has been found specifically to ubiquitylate mutant SOD1 proteins as well as to attenuate mutant SOD-associated toxicity in cultured neuronal cells (Niwa et al., 2002).

NEDL1, a HECT type E3 ligase, has also been reported to be a mutant SOD1-specific E3 ligase and to interact with TRAPδ and dvl1 (Miyazaki et al., 2004). It has also been reported that ubiquitylation of mutant SOD1-associated complex was enhanced by CHIP and Hsp70 *in vivo* (Urushitani et al., 2004). CHIP ubiquitylated Hsp70-holding SOD1 complexes and degraded mutant SOD1, but did not directly interact with mutant SOD1 (Urushitani et al., 2004). Among these E3 molecules, Dorfin seems to be the most potentially beneficial E3 protein for use in ALS therapy since it is the only one that has been demonstrated to reverse mutant SOD1-associated toxicity (Niwa et al., 2002). Furthermore, Dorfin has been localized in various ubiquitin-positive inclusions such as Lewy bodies (LB) in PD, as well as LB-like inclusions in sporadic ALS and glial cell bodies in multiple-system atrophy. These findings indicate that Dorfin may be involved in the pathogenesis of a broad spectrum of neurodegenerative disorders other than familial ALS (Hishikawa et al., 2003; Ito et al., 2003; Ishigaki et al., 2004).

The half-life of Dorfin^{WT} is, however, less than 1 h (Fig. 1, Table 1). The amount of Dorfin is increased in the presence of MG132, a proteasome inhibitor, indicating that Dorfin is immediately degraded in the UPS. Since the nonfunctional RING mutant form of Dorfin, Dorfin$^{C132S/C135S}$, degraded more slowly than did Dorfin^{WT}, Dorfin seemed to be degraded by auto-ubiquitylation. The degradation of Dorfin$^{C132S/C135S}$ is also inhibited by MG132, suggesting that it is degraded by endogenous Dorfin or other E3s. This immediate degradation of Dorfin is a serious problem for its therapeutic application against neurodegenerative diseases.

Several reports have shown that engineered chimera E3s are able to degrade certain substrates with high efficiency. Protac, a chimeric protein-targeting molecule, was designed to target methionine aminopeptidase-2 to Skp1-Cullin-F box complex (SCF) ubiquitin ligase complex for ubiquitylation and degradation (Sakamoto et al.,

Fig. 7. Dorfin-CHIP chimeric proteins can attenuate toxicity induced by mutant SOD1 and decrease the formation of visible aggregation of mutant SOD1 in N2a cells. (A) N2a cells were grown in 96 collagen-coated wells (5000 cells per well) and transfected with 0.15 μg of SOD1^{WT} and 0.05 μg of Mock or 0.15 μg of SOD1^{G85R} and 0.05 μg of Mock, Dorfin, CHIP, or Dorfin-CHIP^{L}. After the medium was changed, MTS assays were done at 48 h of incubation. Viability was measured as the level of absorbance (490 nm). Values are the means±SE, $n=6$. Statistics were carried out by one-way ANOVA. There were significant differences between SOD1^{G85R}-expressing cells coexpressed with Mock and SOD1^{G85R}-expressing cells coexpressed with Dorfin ($p<0.001$), as well as between SOD1^{G85R}-expressing cells coexpressed with Dorfin and SOD1^{G85R}-expressing cells coexpressed with Dorfin-CHIP^{L} ($p<0.001$). (B) N2a cells were transiently expressed with SOD1^{G85R}-GFP and Mock, Dorfin, CHIP, or Dorfin-CHIP^{L}. Immunostaining with anti-FLAG antibody revealed that Dorfin, CHIP, and Dorfin-CHIP^{L} were localized with SOD1^{G85R}-GFP in macroaggresomes (arrows). Scale bar=20 μm (C) The visible macroaggregations in N2a cells expressing both SOD1^{G85R}-GFP and Mock, Dorfin, CHIP, or Dorfin-CHIP^{L} with or without MG132 treatment were counted and the ratio of cells with aggregations to those with GFP signals was calculated. Values are the means±SE, $n=4$. Statistics were done by one-way ANOVA. *$p<0.01$ denotes a significant difference between cells with Mock and Dorfin or Dorfin-CHIP^{L}. **$p<0.05$ denotes a significant difference between cells with Dorfin and Dorfin-CHIP^{L}.

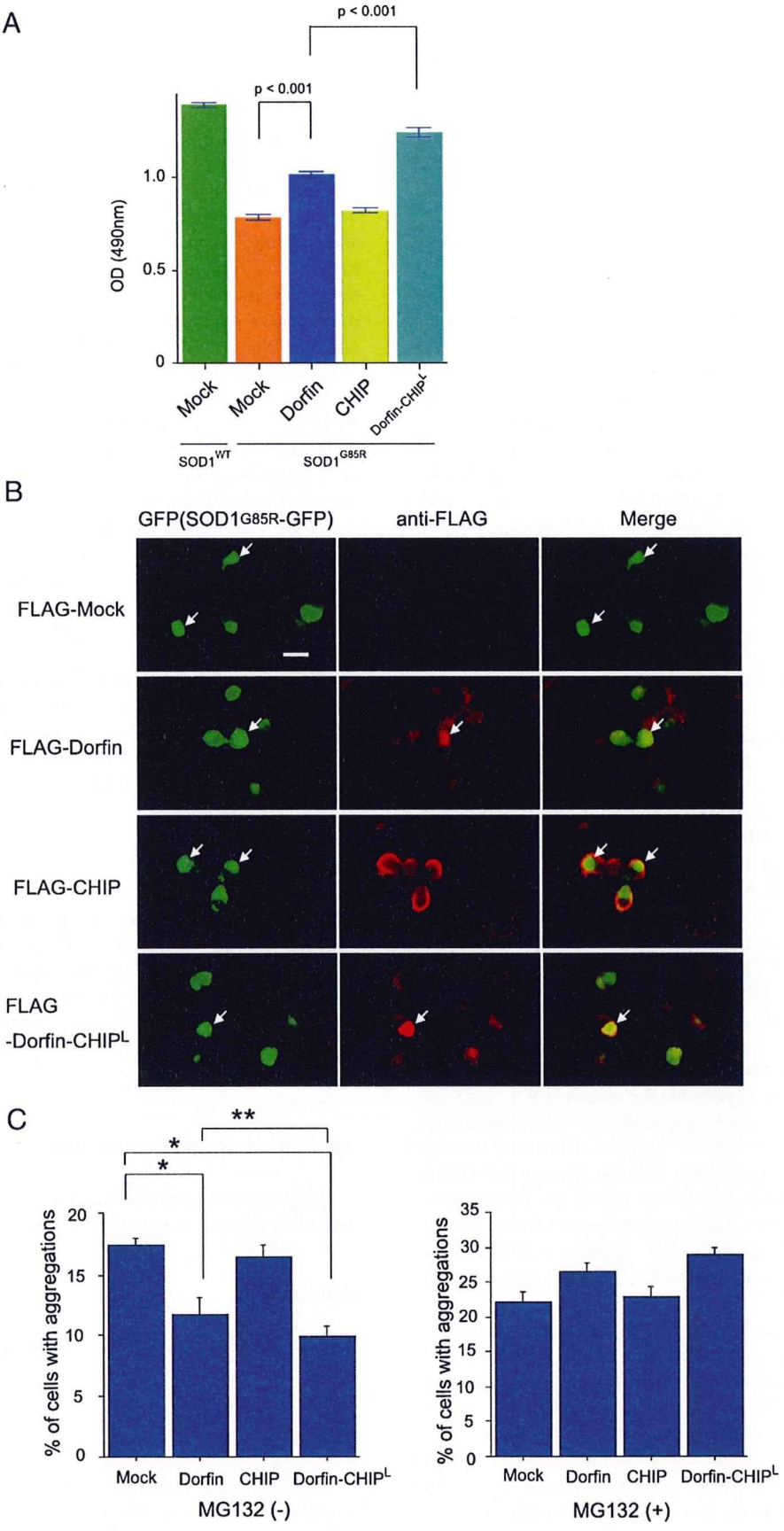
A
p < 0.001
p < 0.001
OD (490nm)
1.0
0.5
0
Mock
Mock
Dorfin
CHIP
Dorfin-CHIP^L
SOD1^WT
SOD1^G85R
B
GFP(SOD1G85R-GFP)
anti-FLAG
Merge
FLAG-Mock
FLAG-Dorfin
FLAG-CHIP
FLAG
-Dorfin-CHIP^L
C
**
*
*
% of cells with aggregations
20
15
10
5
0
Mock
Dorfin
CHIP
Dorfin-CHIP^L
MG132 (-)
35
30
25
20
15
10
5
0
MG132 (+)

2001, 2003). Oyake et al. (2002) developed double RING ubiquitin ligases containing the RING finger domains of both BRCA and BARD1 linked to a substrate recognition site PCNA. Recently, Hatakeyama et al. developed a fusion protein composed of Max, which forms a heterodimer with c-Myc, and the U-box of CHIP. This fusion protein physically interacted with c-Myc and promoted the ubiquitylation of c-Myc. It also reduced the stability of c-Myc, resulting in the suppression of transcriptional activity dependent on c-Myc and the inhibition of tumorogenesis (Hatakeyama et al., 2005). This indicated that the U-box portion of CHIP is able to add an effective E3 function to a U-box-containing client protein.

We postulated that engineered forms of Dorfin could be stable and still function as specific E3s for mutant SOD1s. Dorfin has a RING/IBR domain in the N-terminal portion (amino acids 1-332), but has no obvious motif in the rest of the C-terminus (amino acids 333–838). In this study, we have demonstrated that the hydrophobic domain of Dorfin (amino acids 333–454) is both necessary and sufficient for substrate recruiting (Fig. 2B). In our engineered proteins, the RING/IBR motif of N-terminal Dorfin was replaced by the UPR domain of CHIP, which had strong E3 activity (Murata et al., 2001). Some of the engineered Dorfin-chimeric proteins, such as Dorfin-CHIP$^{D, G, J}$, and ^{L}, were degraded *in vivo* far more slowly than was wild-type Dorfin, indicating that they were capable of being stably presented *in vivo* (Fig. 3). However, Dorfin-CHIP^{G} failed to show strong ubiquitylation activity against SOD1^{G85R} in HEK293 cells. Since Dorfin-CHIP$^{D, J}$, and ^{L} were able to bind to SOD1^{G85R} more strongly than did Dorfin-CHIP^{G}, the binding activity was more important for the E3 activity than for the protein stability.

We next showed that although all of the Dorfin-CHIP chimeric proteins bound to mutant SOD1 *in vivo*, some of them, such as Dorfin-CHIP$^{B, C}$, and ^{I}, bound less than others (Fig. 4A). In HEK293 cells, Dorfin-CHIP$^{D, E, F, J, K}$, and ^{L} ubiquitylated SOD1^{G85R} more effectively than did Dorfin or CHIP; however, in N2a cells only Dorfin-CHIP^{L} had more effective E3 activity than did Dorfin or CHIP. This discrepancy may be due to differences between HEK 293 and N2a cells which could provide slight different environment for the E3 machinery. Therefore, Dorfin-CHIP^{L} was the most potent of the candidate chimeric proteins in degrading mutant SOD1 in the UPS in neuronal cells. We also showed that Dorfin-CHIP^{L} could specifically bind to and ubiquitylate mutant SOD1s but not SOD1^{WT} *in vivo*, as Dorfin had done (Niwa et al., 2002; Ishigaki et al., 2004) (Fig. 5). This observation confirmed that the hydrophobic domain of Dorfin (amino acids 333–454) is responsible for mutant SOD1 recruiting.

Pulse-chase analysis using N2a cells showed that Dorfin-CHIP^{L} degraded SOD1^{G85R} and SOD1^{G93A} more effectively than did Dorfin (Fig. 6). This is compatible with the finding that Dorfin-CHIP^{L} had a greater effect than Dorfin did on the ubiquitylation against mutant SOD1. The cycloheximide assay verified that the degradation ability of Dorfin-CHIP^{L} against SOD1^{G85R} was stronger than that of Dorfin or CHIP in HEK293 cells (data not shown).

Dorfin-CHIP^{L} also reversed SOD1^{G85R}-associated toxicity in N2a cells more effectively than did Dorfin (Fig. 7). This therapeutic effect of Dorfin-CHIP^{L} was expected from its strong E3 activity and degradation ability against SOD1^{G85R}. Visible protein aggregations have been considered to be hallmarks of neurodegeneration. Increased understanding of the pathway involved in protein aggregation may demonstrate that visible macroaggregates represent the end-stage of a molecular cascade of steps rather than a direct toxic insult (Ross and Poirier, 2004). Two facts that Dorfin-CHIP^{L} decreased aggregation formation of SOD1^{G85R} and that this effect was inhibited by a proteasome inhibitor should reflect the ability of Dorfin-CHIP^{L} to degrade mutant SOD1 in the UPS of cells.

Based on our present observations, Dorfin-CHIP^{L}, an engineered chimeric molecule with the hydrophobic substrate-binding domain of Dorfin and the U-box domain of CHIP, had stronger E3 activity against mutant SOD1 than did Dorfin or CHIP. Indeed, it not only degraded mutant SOD1 more effectively than did Dorfin or CHIP but, as compared to Dorfin, produced marked attenuation of mutant SOD1-associated toxicity in N2a cells. This protective effect of Dorfin-CHIP^{L} against mutant SOD1 has potential applications to gene therapy for mutant SOD1 transgenic mice because this protein has a long enough life to allow the constant removal of mutant SOD1 from neurons. Since Dorfin was originally identified as a sporadic ALS-associated molecule (Ishigaki et al., 2002b) and is located in the ubiquitin-positive inclusions of various neurodegenerative diseases (Hishikawa et al., 2003), this molecule is an appropriate candidate for future use in gene therapy not only for familial ALS, but also for sporadic ALS and other neurodegenerative disorders.

So far, most reports on engineered chimera E3s have targeted cancer-promoting proteins. Dorfin-CHIP chimeric proteins are the first chimera E3s to be intended for the treatment of neurodegenerative diseases. Since the accumulation of ubiquitylated proteins in neurons is a pathological hallmark of various neurodegenerative diseases, development of chimera E3s like Dorfin-CHIP^{L}, which can remove unnecessary proteins, is a new therapeutic concept. Further analysis, including transgenic overexpression and vector delivery of Dorfin-CHIP chimeric proteins using ALS animal models will increase our understanding of the potential utility of Dorfin-CHIP chimeric proteins as therapeutic tools.

Acknowledgments

We gratefully thank Dr. Shigetsugu Hatakeyama at Hokkaido University for his advice about the construction of Dorfin-CHIP chimeric proteins. This work was supported by the Nakabayashi Trust for ALS Research; a grant for Center of Excellence (COE) from the Ministry of Education, Culture, Sports, Science and Technology of Japan; and grants from the Ministry of Health, Welfare and Labor of Japan.

Appendix A. Supplementary data

Supplementary data associated with this article can be found, in the online version, at doi:10.1016/j.nbd.2006.09.017.

References

Alves-Rodrigues, A., Gregori, L., Figueiredo-Pereira, M.E., 1998. Ubiquitin, cellular inclusions and their role in neurodegeneration. Trends Neurosci. 21, 516–520.

Bercovich, B., Stancovski, I., Mayer, A., Blumenfeld, N., Laszlo, A., Schwartz, A.L., Ciechanover, A., 1997. Ubiquitin-dependent degradation of certain protein substrates in vitro requires the molecular chaperone Hsc70. J. Biol. Chem. 272, 9002–9010.

Ciechanover, A., Brundin, P., 2003. The ubiquitin proteasome system in

neurodegenerative diseases: sometimes the chicken, sometimes the egg. Neuron 40, 427–446.

Cudkowicz, M.E., McKenna-Yasek, D., Sapp, P.E., Chin, W., Geller, B., Hayden, D.L., Schoenfeld, D.A., Hosler, B.A., Horvitz, H.R., Brown, R.H., 1997. Epidemiology of mutations in superoxide dismutase in amyotrophic lateral sclerosis. Ann. Neurol. 41, 210–221.

Glickman, M.H., Ciechanover, A., 2002. The ubiquitin–proteasome proteolytic pathway: destruction for the sake of construction. Physiol. Rev. 82, 373–428.

Hatakeyama, S., Matsumoto, M., Kamura, T., Murayama, M., Chui, D.H., Planel, E., Takahashi, R., Nakayama, K.I., Takashima, A., 2004. U-box protein carboxyl terminus of Hsc70-interacting protein (CHIP) mediates poly-ubiquitylation preferentially on four-repeat Tau and is involved in neurodegeneration of tauopathy. J. Neurochem. 91, 299–307.

Hatakeyama, S., Watanabe, M., Fujii, Y., Nakayama, K.I., 2005. Targeted destruction of c-Myc by an engineered ubiquitin ligase suppresses cell transformation and tumor formation. Cancer Res. 65, 7874–7879.

Hishikawa, N., Niwa, J., Doyu, M., Ito, T., Ishigaki, S., Hashizume, Y., Sobue, G., 2003. Dorfin localizes to the ubiquitylated inclusions in Parkinson's disease, dementia with Lewy bodies, multiple system atrophy, and amyotrophic lateral sclerosis. Am. J. Pathol. 163, 609–619.

Ishigaki, S., Liang, Y., Yamamoto, M., Niwa, J., Ando, Y., Yoshihara, T., Takeuchi, H., Doyu, M., Sobue, G., 2002a. X-Linked inhibitor of apoptosis protein is involved in mutant SOD1-mediated neuronal degeneration. J. Neurochem. 82, 576–584.

Ishigaki, S., Niwa, J., Ando, Y., Yoshihara, T., Sawada, K., Doyu, M., Yamamoto, M., Kato, K., Yotsumoto, Y., Sobue, G., 2002b. Differentially expressed genes in sporadic amyotrophic lateral sclerosis spinal cords—Screening by molecular indexing and subsequent cDNA microarray analysis. FEBS Lett. 531, 354–358.

Ishigaki, S., Hishikawa, N., Niwa, J., Iemura, S., Natsume, T., Hori, S., Kakizuka, A., Tanaka, K., Sobue, G., 2004. Physical and functional interaction between Dorfin and Valosin-containing protein that are colocalized in ubiquitylated inclusions in neurodegenerative disorders. J. Biol. Chem. 279, 51376–51385.

Ito, T., Niwa, J., Hishikawa, N., Ishigaki, S., Doyu, M., Sobue, G., 2003. Dorfin localizes to Lewy bodies and ubiquitylates synphilin-1. J. Biol. Chem. 278, 29106–29114.

Johnston, J.A., Ward, C.L., Kopito, R.R., 1998. Aggresomes: a cellular response to misfolded proteins. J. Cell Biol. 143, 1883–1898.

Julien, J.P., 2001. Amyotrophic lateral sclerosis. unfolding the toxicity of the misfolded. Cell 104, 581–591.

Jungmann, J., Reins, H.A., Schobert, C., Jentsch, S., 1993. Resistance to cadmium mediated by ubiquitin-dependent proteolysis. Nature 361, 369–371.

Lee, D.H., Sherman, M.Y., Goldberg, A.L., 1996. Involvement of the molecular chaperone Ydj1 in the ubiquitin-dependent degradation of short-lived and abnormal proteins in *Saccharomyces cerevisiae*. Mol. Cell. Biol. 16, 4773–4781.

Meacham, G.C., Patterson, C., Zhang, W., Younger, J.M., Cyr, D.M., 2001. The Hsc70 co-chaperone CHIP targets immature CFTR for proteasomal degradation. Nat. Cell Biol. 3, 100–105.

Miyazaki, K., Fujita, T., Ozaki, T., Kato, C., Kurose, Y., Sakamoto, M., Kato, S., Goto, T., Itoyama, Y., Aoki, M., Nakagawara, A., 2004. NEDL1, a novel ubiquitin–protein isopeptide ligase for dishevelled-1, targets mutant superoxide dismutase-1. J. Biol. Chem. 279, 11327–11335.

Murata, S., Minami, Y., Minami, M., Chiba, T., Tanaka, K., 2001. CHIP is a chaperone-dependent E3 ligase that ubiquitylates unfolded protein. EMBO Rep. 2, 1133–1138.

Murata, S., Chiba, T., Tanaka, K., 2003. CHIP: a quality-control E3 ligase collaborating with molecular chaperones. Int. J. Biochem. Cell Biol. 35, 572–578.

Niwa, J., Ishigaki, S., Doyu, M., Suzuki, T., Tanaka, K., Sobue, G., 2001. A novel centrosomal ring-finger protein, dorfin, mediates ubiquitin ligase activity. Biochem. Biophys. Res. Commun. 281, 706–713.

Niwa, J., Ishigaki, S., Hishikawa, N., Yamamoto, M., Doyu, M., Murata, S., Tanaka, K., Taniguchi, N., Sobue, G., 2002. Dorfin ubiquitylates mutant SOD1 and prevents mutant SOD1-mediated neurotoxicity. J. Biol. Chem. 277, 36793–36798.

Oyake, D., Nishikawa, H., Koizuka, I., Fukuda, M., Ohta, T., 2002. Targeted substrate degradation by an engineered double RING ubiquitin ligase. Biochem. Biophys. Res. Commun. 295, 370–375.

Rosen, D.R., Siddique, T., Patterson, D., Figlewicz, D.A., Sapp, P., Hentati, A., Donaldson, D., Goto, J., O'Regan, J.P., Deng, H.X., et al., 1993. Mutations in Cu/Zn superoxide dismutase gene are associated with familial amyotrophic lateral sclerosis. Nature 362, 59–62.

Ross, C.A., Poirier, M.A., 2004. Protein aggregation and neurodegenerative disease. Nat. Med. 10, S10–S17 (Suppl.).

Rowland, L.P., Shneider, N.A., 2001. Amyotrophic lateral sclerosis. N. Engl. J. Med. 344, 1688–1700.

Sakamoto, K.M., Kim, K.B., Kumagai, A., Mercurio, F., Crews, C.M., Deshaies, R.J., 2001. Protacs: chimeric molecules that target proteins to the Skp1-Cullin-F box complex for ubiquitination and degradation. Proc. Natl. Acad. Sci. U. S. A. 98, 8554–8559.

Sakamoto, K.M., Kim, K.B., Verma, R., Ransick, A., Stein, B., Crews, C.M., Deshaies, R.J., 2003. Development of Protacs to target cancer-promoting proteins for ubiquitination and degradation. Mol. Cell Proteomics 2, 1350–1358.

Scheffner, M., Nuber, U., Huibregtse, J.M., 1995. Protein ubiquitination involving an E1–E2–E3 enzyme ubiquitin thioester cascade. Nature 373, 81–83.

Sherman, M.Y., Goldberg, A.L., 2001. Cellular defenses against unfolded proteins: a cell biologist thinks about neurodegenerative diseases. Neuron 29, 15–32.

Shimura, H., Schwartz, D., Gygi, S.P., Kosik, K.S., 2004. CHIP–Hsc70 complex ubiquitinates phosphorylated tau and enhances cell survival. J. Biol. Chem. 279, 4869–4876.

Tanaka, K., Suzuki, T., Hattori, N., Mizuno, Y., 2004. Ubiquitin, proteasome and parkin. Biochim. Biophys. Acta 1695, 235–247.

Urushitani, M., Kurisu, J., Tateno, M., Hatakeyama, S., Nakayama, K., Kato, S., Takahashi, R., 2004. CHIP promotes proteasomal degradation of familial ALS-linked mutant SOD1 by ubiquitinating Hsp/Hsc70. J. Neurochem. 90, 231–244.

Yoshida, Y., Tokunaga, F., Chiba, T., Iwai, K., Tanaka, K., Tai, T., 2003. Fbs2 is a new member of the E3 ubiquitin ligase family that recognizes sugar chains. J. Biol. Chem. 278, 43877–43884.

Clin Auton Res (2007) 17:20–25
DOI 10.1007/s10286-006-0378-8

RESEARCH ARTICLE

Motoko Takamori
Masaaki Hirayama
Rei Kobayashi
Hiroki Ito
Naoki Mabuchi
Tomohiko Nakamura
Norio Hori
Yasuo Koike
Gen Sobue

Altered venous capacitance as a cause of postprandial hypotension in multiple system atrophy

Accepted: 16 October 2006
Published online: 29 November 2006

M. Takamori, MD · M. Hirayama, MD
H. Ito, MD · T. Nakamura, MD
N. Hori, MD · G. Sobue, MD (✉)
Dept. of Neurology
Nagoya University Graduate School of Medicine
Nagoya 466-8550, Japan
Tel.: +81-52/744-2385
Fax: +81-52/744-2384
E-Mail: sobueg@med.nagoya-u.ac.jp

R. Kobayashi, MD
Dept. of Neurology
Nagoya Medical Center
Nagoya, Japan

N. Mabuchi, MD
Dept. of Neurology
Okazaki Municipal Hospital
Aichi, Japan

Y. Koike, MD
Dept. of Health Science
Nagoya University Graduate School of Medicine
Nagoya, Japan

Abstract Patients with multiple system atrophy (MSA) often have clinically significant postprandial hypotension (PPH). To elucidate the cause of insufficient cardiac preload augmentation that underlies PPH, we recorded calf venous capacitance (CVC) by strain-gauge plethysmography, in 17 MSA patients and eight healthy controls before and after oral glucose ingestion. Among 17 MSA patients, nine who showed a decrease in systolic blood pressure exceeding 20 mmHg and were diagnosed with PPH. MSA patients without PPH showed a significant decrease in CVC and a significant increase in cardiac output after oral glucose ingestion, as did controls; those with MSA exhibiting PPH showed a significant increase in CVC and no significant change in cardiac output. The change in CVC correlated positively with the decrease in systolic and diastolic blood pressure after glucose ingestion, and also correlated negatively with the increase in cardiac output. Physiologically, PPH is prevented by a decrease in venous capacitance, which increases circulating blood volume and cardiac output. In some MSA patients, failure of venous capacitance to decrease may induce PPH.

Key words postprandial · hypotension · multiple system atrophy · venous capacitance · autonomic nervous system

Introduction

Postprandial hypotension (PPH) was first reported as a clinical problem in a patient with parkinsonism [20], although a change in blood pressure provoked by eating already had been recognized [5, 21]. Currently PPH is known to occur frequently among patients with autonomic failure caused by multiple system atrophy (MSA), pure autonomic failure (PAF) [16, 17], Parkinson's disease [18, 25], and diabetes mellitus [13]; PPH even may occur in hypertensive patients and healthy elderly subjects [14]. Like orthostatic hypotension (OH), PPH can be a major clinical problem because of various alarming, sometimes serious symptoms such as dizziness, nausea, lightheadedness, weakness, syncope, falls, angina pectoris, and cerebral ischemia [13, 26]. Various reported studies have sought to clarify the mechanism of PPH. Food ingestion increases portal blood flow

CAR 378

and may cause hypotension [19, 24]. In normal healthy subjects, cardiac output increases postprandially while blood pressure does not decrease; in patients with PPH, cardiac output fails to increase [10, 16]. Cardiac output can be increased by increasing preload (venous return), decreasing afterload (systemic vascular resistance), and/or increasing myocardial contractility (β1 sympathetic stimulation). In a previous study, we found decreased afterload (vascular resistance) in PPH despite unchanged cardiac output, while healthy controls showed a postprandial increase in cardiac output in the absence of a significant increase in heart rate (HR) [6, 10]. If myocardial contractility augmentation by β1 sympathetic excitation were a major contribution to the normal postprandial increase in cardiac output, HR would be expected to increase more. Based on these observations, we hypothesized that the preloading effect of venous compliance is a crucial physiologic factor preventing PPH. However, no reported studies or anecdotal accounts have described venous compliance in patients with PPH. Venous compliance is pressure dependent value, so the measurement of venous compliance needs frequent examinations and takes some times [7, 23], and standard methods have not been established. PPH is a phenomenon which changes in minutes, so the measurement of venous compliance is difficult in PPH. We therefore substituted calf venous capacitance (CVC) for venous compliance [3], assessing its involvement in the pathophysiology of PPH.

Table 1 Clinical features and autonomic function parameters in MSA patients with PPH, MSA patients without PPH, and controls

	MSA with PPH (n = 9)	MSA without PPH (n = 8)	Controls (n = 8)
Age (years)	59.6 (9.0)	60.5 (8.3)	48.6 (10.2)
Gender (M:F)	4:5	5:3	7:1
Disease duration (years)	3.4 (1.6)	4.6 (3.4)	
Baseline			
SBP (mmHg)	147 (18)§	125 (12)	121 (15)
DBP (mmHg)	82 (9)	78 (6)	70 (11)
HR (bpm)	74 (12)	71 (9)	71 (10)
Clinical PPH	2/9 (22%)	0/8 (0%)	0/8 (0%)
Change after glucose ingestion			
• SBP (mmHg)	−35 (12)†	−2 (5)	0 (7)
• DBP (mmHg)	−21 (7)†	−6 (6)	1 (6)
• HR (bpm)	4 (6)	1 (4)	−1 (5)
OH	9/9 (100%)*	6/8 (75%)**	0/8 (0%)
Clinical OH	7/9 (78%)‡	1/8 (13%)	0/8 (0%)
Change after 60° head up			
• SBP (mmHg)	−47 (20)*	−29 (22)***	−3 (9)
• DBP (mmHg)	−25 (11)*	−12 (21)	1 (6)
NE supersensitivity	8/9 (89%)	4/8 (50%)	n.e.
Change after NE infusion			
• SBP (mmHg)	31 (6)	23 (15)	n.e.
• DBP (mmHg)	19 (10)	13 (17)	n.e.
NE (pmol/l)	992 (610)	1520 (654)	1778 (824)
AVP (pg/ml)	1.83 (1.57)	0.98 (0.64)	1.22 (0.70)

*p < 0.001 vs. controls. **p < 0.01 vs. controls. ***p < 0.05 vs. controls. $^{\dagger}p$ < 0.001 vs. both MSA without PPH and controls. $^{\ddagger}p$ < 0.05 vs. MSA without PPH, <0.001 vs. controls. $^{\S}p$ < 0.05 vs. MSA without PPH, <0.01 vs. controls. MSA, multiple system atrophy; PPH, postprandial hypotension; OH, orthostatic hypotension; NE, norepinephrine; AVP, arginine vasopressin; n.e., not evaluated

Methods

Subjects

The 17 consecutive probable MSA patients participating in this study included nine men and eight women (mean age at examination ± SD, 59.8 ± 7.9 years, range, 46–73; mean illness duration, 4.2 ± 2.6 years, range, 2–10). Probable MSA was diagnosed according to the criteria established by a consensus statement concerning the diagnosis of MSA [4]. Criteria for exclusion from this study were presence of cardiovascular disease, diabetes mellitus, peripheral neuropathy, and severely impaired motor function defined as a Modified Rankin Scale score exceeding 4 (inability to walk independently with or without a crutch). Eight normal healthy control subjects also were studied (Table 1). The ethics committee of the Nagoya University School of Medicine approved this study in full. We obtained informed consent from all subjects prior to study participation.

Glucose loading test

Protocol

The test began at 9:00 AM in our laboratory, at an ambient temperature of 25°C. All medications and oral intake were withheld after the night before the study. Subjects lay supine on a bed and were monitored at rest for 30 min (baseline period), and then for another 30 min after oral ingestion of 75 g of glucose in 225 ml of water. Systolic blood pressure (SBP), diastolic blood pressure (DBP), HR, cardiac output, and arterial blood flow in the lower legs (LBF) were measured continuously. CVC was measured twice, at baseline and at 30 min after glucose ingestion. We defined PPH as a decrease in SBP following glucose administration that exceeded 20 mmHg [13]. Clinical PPH was defined as sensation of dizziness, visual disturbance, or a gradual fading of consciousness after food ingestion during the study or previously.

Hemodynamic measurements

SBP, DBP, and HR were measured in the right radial artery at the wrist by tonometry (BP-508; COLIN, Aichi, Japan), which noninvasively determined the subject's beat-to-beat blood pressure. The electrocardiogram (ECG) was monitored. Cardiac output and LBF were monitored by impedance plethysmograph (4134; NEC San-ei, Tokyo, Japan). CVC was measured using a mercury-filled silastic strain-gauge plethysmograph (EC-5R; Hokanson Inc., Washington, USA). The strain gauge was positioned around the midpoint of the right calf to measure change in lower limb volume. After a blood pressure cuff at the right ankle had been inflated to 200 mmHg and had rendered the sole of the foot temporarily ischemic, a thigh blood pressure cuff was inflated additionally to 40 mmHg for 2 min, while the change in lower limb volume was recorded. CVC was defined as volume increase (ml/100 ml) [2, 3, 12]. CVC was

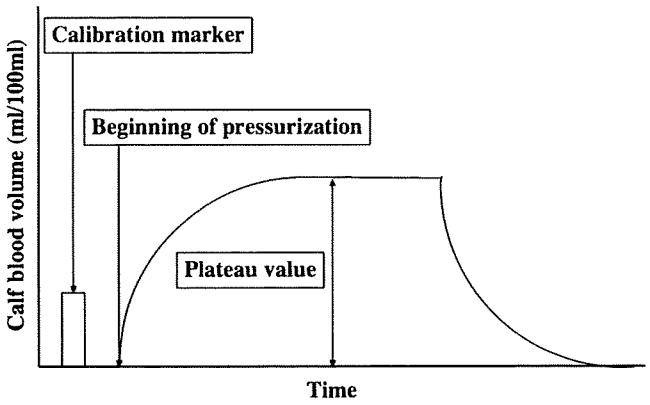

Fig. 1 Illustration of limb volume curve. Calf volume changes following applied thigh blood cuff pressurization. Calf venous capacitance was calculated from plateau value divided by the height of the calibration marker. This marker represents a 1% change in the electrical resistance of the conductor inside the gauge, which is equal to a 1% limb volume

calculated by measuring the plateau value of limb volume curve after thigh blood pressure cuff was inflated to 40 mmHg and dividing this value by the height of calibration marker; this marker represents a 1% change in the electrical resistance of the conductor inside the gauge, which is equal to a 1% change in limb volume (Fig. 1). The change of blood pressure can influence the plateau time, but it does not influence the plateau value except when SBP goes down to less than 40 mmHg. Cardiac output and LBF were presented here as percentage variation from the baseline value, because the measurement of absolute value was not possible by impedance method.

Head-up tilting

On a different day than the hemodynamic tests, head-up tilting was carried out with the subject in a supine position on a tilt table with a foot-plate support. The table was tilted in a stepwise manner (20°, 40°, and 60° for 5 min each). We diagnosed OH when the decrease of SBP during head-up tilting exceeded 20 mmHg, or the decrease of DBP during head-up tilting exceeded 10 mmHg [15]. Clinical OH was defined as sensation of dizziness, visual disturbance, or a gradual fading of consciousness after standing during the study or previously.

Denervation supersensitivity to norepinephrine (NE)

To assess sensitivity to NE, we administered an intravenous NE infusion at a rate of 3 μg/min for 3 min. A diagnosis of the denervation supersensitivity was made when SBP increased more than 25 mmHg [9].

Plasma norepinephrine (NE) and arginine vasopressin (AVP)

To determine plasma NE and AVP, venous blood was sampled after rest in the supine position for at least 30 min.

Both NE infusion tests and examinations of plasma NE and AVP were performed on the same day as head-up tilting. NE infusion tests were not performed in the healthy controls.

Statistical analysis

The Fisher's exact probability test was used to compare the usage of vasopressor between the group with MSA inducing PPH and with MSA without PPH. The Mann–Whiney *U*-test was used to assess differences for continuous variables between the group with MSA inducing PPH and with MSA without PPH. Scheffé's *F*-test was used for post hoc testing between three groups (MSA with PPH, MSA without PPH, and controls). Wilcoxon signed-ranks tests were used to assess differences in cardiac output and CVC between determinations at baseline and after glucose ingestion. Relationships between change in CVC and decrease in SBP and DBP, between change in CVC and increase in cardiac output, were analyzed using Spearman's correlation coefficient by rank. Calculations were performed using the StatView statistical software package (version 5.0; Abacus Concepts, Berkeley, CA). Statistical significance was defined by $p < 0.05$. Values are presented as the means ± SD.

Results

Clinical features and autonomic functions in each group are summarized in Table 1. Of 17 MSA patients, nine were diagnosed with PPH positive, while the other eight were PPH negative. All eight controls were PPH negative.

Clinical features

No significant difference was evident in illness duration or age at examination between the MSA group with PPH and the MSA group without PPH. Controls were slightly younger than subjects in the other two groups, but the age difference was not significant. Four out of nine MSA patients with PPH took vasopressor before the examination. One took droxidopa, one amezium, one took both droxidopa and midodrine, and another both droxidopa and amezium. Only one out of eight MSA patients without PPH took vasopressor, both doroxidopa and midodrine before the examination. More patients with PPH used vasopressor than patients without PPH, although the difference was not significant.

Response to glucose loading test

SBP at baseline in MSA with PPH was significantly higher than in MSA without PPH or in controls ($p < 0.05$ and $p < 0.01$, respectively). DBP or HR at baseline was not significantly different between MSA with PPH, MSA without PPH, and controls. The change in SBP after glucose ingestion in MSA with PPH was significantly greater than in MSA without PPH or in controls (both $p < 0.001$). The change in DBP after glucose ingestion in MSA with PPH was

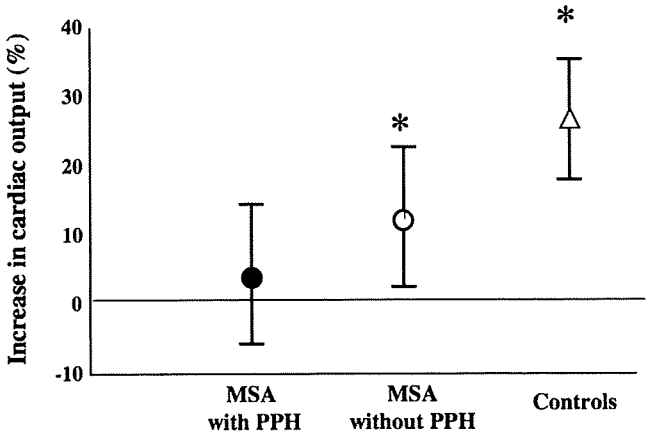

Fig. 2 Increase in cardiac output after glucose ingestion in multiple system atrophy (MSA) patients with postprandial hypotension (PPH), MSA patients without PPH, and normal control subjects. Values are means, with error bars indicating SD. *$p < 0.05$ vs. baseline

significantly greater than in MSA without PPH or in controls (both $p < 0.001$). The change in HR after glucose ingestion was not significantly different between the three groups (Table 1).

Cardiac output increased significantly in MSA without PPH (13 ± 10%, $p < 0.05$) and in controls (26 ± 9%, $p < 0.05$), while output did not change significantly in MSA with PPH (4 ± 10%; Fig. 2). After glucose ingestion, CVC decreased significantly in MSA without PPH (from 2.20 ± 0.88% to 1.84 ± 0.60%, $p < 0.05$) and in controls (from 2.04 ± 0.24% to 1.72 ± 0.36%, $p < 0.05$), but increased significantly in MSA with PPH (from 1.80 ± 0.72% to 2.08 ± 0.88%, $p < 0.05$; Fig. 3). The change in CVC correlated positively with the decrease

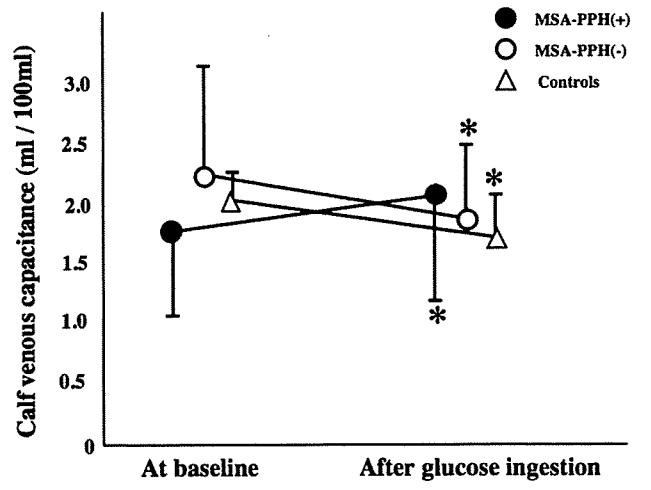

Fig. 3 Change in calf venous capacitance after glucose ingestion in multiple system atrophy (MSA) patients with postprandial hypotension (PPH), MSA patients without PPH, and normal control subjects. Values are means, with error bars indicating SD. *$p < 0.05$ vs. baseline

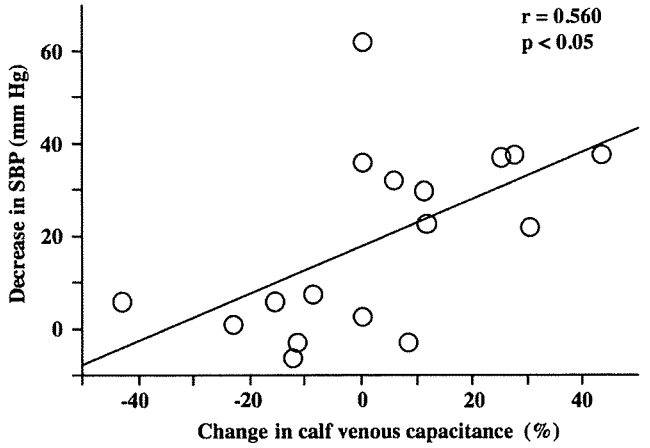

Fig. 4 Change in calf venous capacitance showed significant positive correlation with decrease in systolic blood pressure (SBP) after glucose ingestion across the whole MSA population ($r = 0.560$, $p < 0.05$)

in SBP ($r = 0.560$, $p < 0.05$; Fig. 4), and with the decrease in DBP ($r = 0.524$, $p < 0.05$; Fig. 5) after glucose ingestion, and correlated negatively with the increase in cardiac output ($r = -0.583$, $p < 0.05$; Fig. 6). The increases of LBF after glucose ingestion were 1 ± 19% in MSA with PPH, 0 ± 37% in MSA without PPH, and 3 ± 9% in controls, and there were no significant differences among three groups.

Other autonomic function tests

All nine MSA patients with PPH demonstrated OH. Frequency of OH in MSA with PPH (100%) and in MSA without PPH (75%) was significantly higher than in controls (0%); ($p < 0.001$, $p < 0.01$, respectively).

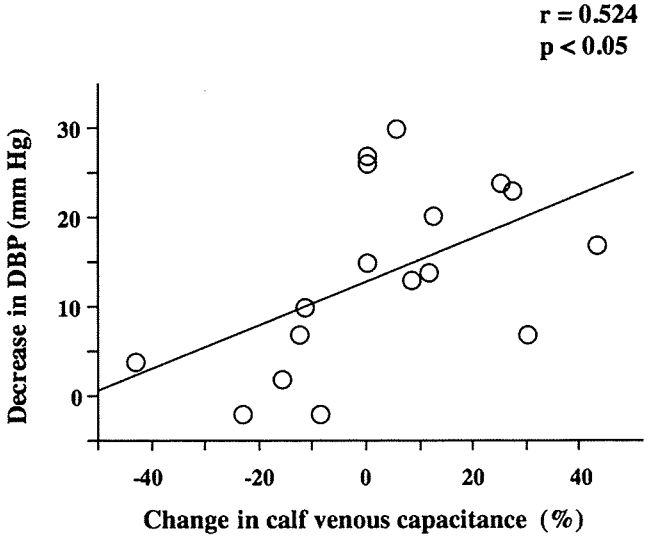

Fig. 5 Change in calf venous capacitance showed significant positive correlation with decrease in diastolic blood pressure (DBP) after glucose ingestion across the whole MSA population ($r = 0.524$, $p < 0.05$)

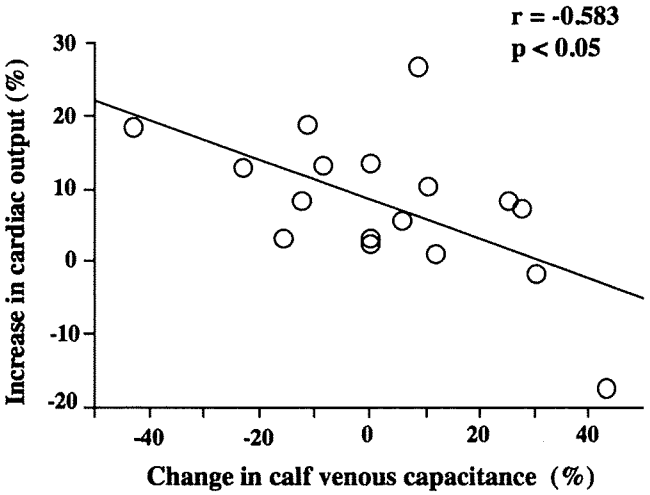

Fig. 6 Change in calf venous capacitance showed significant negative correlation with increase in cardiac output after glucose ingestion across the whole MSA population ($r = -0.583$, $p < 0.05$)

Frequency of OH was slightly higher in MSA with PPH than in MSA without PPH, but the difference was not significant. NE supersensitivity was demonstrated more frequently in MSA with PPH than in MSA without PPH, but the difference was not significant. Plasma NE was slightly lower in MSA with PPH than in MSA without PPH or in controls, but the difference was not significant. Plasma NE levels were not significantly correlated with HR and with CVC changes after glucose ingestion across the whole MSA population. Plasma AVP in MSA with PPH was slightly but not significantly higher than in MSA without PPH or in controls (Table 1).

Discussion

Reduced CVC and increased cardiac output after glucose ingestion were demonstrated in MSA without PPH and in controls, while in contrast CVC increased after ingestion in MSA with PPH. The change in CVC showed a negative correlation with the increase in cardiac output. Furthermore, the change in CVC after glucose ingestion correlated positively with the decrease in SBP and DBP. The venous system has been found to normally contain 64% of total blood volume while showing great distensibility, as to represent a reserve compartment for circulating blood volume [22]. Regulation of venous capacitance thus plays an important role in homeostasis of the systemic circulation system. A reduction of venous capacitance increases effective intravascular volume that results in an increase in cardiac output. A physiologic decline in venous capacitance can contribute importantly to systemic compensation for increased splanchnic blood flow induced by a meal; failure of venous capacitance reduction to occur is one of the factors underlying PPH, especially in MSA.

The precise mechanism of PPH has not been fully clarified. As presently understood, the causative sequence would begin with food ingestion inducing an increase in splanchnic blood flow [19, 24], and release of vasodilatory gastrointestinal peptides such as neurotensin [1, 8, 16]; as a result, systemic blood pressure tends to decrease. In normal subjects, the sympathetic nervous system is then activated to prevent systemic hypotension. However, this compensatory system is compromised in patients with autonomic failure, this defect eventually can result in PPH. Previous studies have shown evidence of impaired sympathetic compensation in PPH patients, including diminished baroreflex function, blunted compensatory increases in cardiac output, impairment of physiologic increases in muscle sympathetic nerve activity [6], and insufficient peripheral vasoconstriction [10, 13, 16]. These response defects are compatible with our previous finding that simultaneous treatment with β_1 and α_1 agonists sufficiently increased cardiac output and vascular resistance to prevent PPH [11]. The present study implicates defective regulation of venous capacitance as an important contributor to PPH. A notable finding in this study is that CVC after glucose ingestion not only failed to decrease, but actually increased in MSA with PPH. The mechanism resulting in elevation is not clear, and further studies are necessary.

In this study HR did not change in MSA patients, even when SBP decreased significantly. This compromised physiologic response suggests that impaired baroreflex function also contributes to PPH in MSA. Thus, PPH appears to result from an interplay of several mechanisms.

MSA with PPH showed somewhat more frequent NE supersensitivity than MSA without PPH, while falling short of significance. NE denervation supersensitivity suggests that postganglionic sympathetic neurons are affected in this MSA subgroup. Thus, MSA with PPH had more severely impaired autonomic function than MSA without PPH. As the illness progresses, MSA patients have increasing difficulty maintaining an upright posture, so PPH becomes a more troublesome symptom than OH. The frequency of clinical PPH was low even in the group diagnosed as PPH by glucose loading test. PPH is a symptom that patients often fail to notice, although it can lead to severe clinical problems such as cardiac and cerebral ischemia [13, 26]. Not only patients but also caregivers and health care staffs need to keep alert to possible consequences of PPH.

References

1. Carraway R, Leeman SE (1973) The isolation of a new hypotensive peptide, neurotensin, from bovine hypothalami. J Biol Chem 248:6854–6861
2. Forconi S, Jageneau A, Guerrini M, Pecchi S, Cappelli R (1979) Strain gauge plethysmography in the study of circulation of the limbs. Angiology 30:487–497
3. Fu Q, Iwase S, Niimi Y, Kamiya A, Michikami D, Mano T, Suzumura A (2002) Age-related influences of leg vein filling and emptying on blood volume redistribution and sympathetic reflex during lower body negative pressure in humans. Jpn J Physiol 52:77–84
4. Gilman S, Low PA, Quinn N, Albanese A, Ben-Shlomo Y, Fowler CJ, Kaufmann H, Klockgether T, Lang AE, Lantos PL, Litvan I, Mathias CJ, Oliver E, Robertson D, Schatz I, Wenning GK (1999) Consensus statement on the diagnosis of multiple system atrophy. J Neurol Sci 163:94–98
5. Gladstone SA (1935) Cardiac output and related functions under basal and postprandial conditions. Arch Intern Med 55:533–546
6. Hakusui S, Sugiyama Y, Iwase S, Hasegawa Y, Koike Y, Mano T, Takahashi A (1991) Postprandial hypotension: microneurographic analysis and treatment with vasopressin. Neurology 41:712–715
7. Halliwill JR, Minson CT, Joyner MJ (1999) Measurement of limb venous compliance in humans: technical considerations and physiological findings. J Appl Physiol 87:1555–1563
8. Hirayama M, Ieda T, Koike Y, Takeuchi Y, Takeuchi S, Sakurai N, Hakusui S, Hasegawa Y, Takahashi A (1994) Pathophysiology of postprandial hypotension in patients with progressive autonomic failure (6)—comparison of gut peptide responses to oral intake of glucose and protein. Auton Nerv Syst 31:47–51
9. Hirayama M, Koike Y (1997) Pharmacological test. Nippon Rinsho 55(Suppl 1):491–493
10. Hirayama M, Watanabe H, Koike Y, Hasegawa Y, Kanaoke Y, Sakurai N, Hakusui S, Takahashi A (1993) Postprandial hypotension: hemodynamic differences between multiple system atrophy and peripheral autonomic neuropathy. J Auton Nerv Syst 43:1–6
11. Hirayama M, Watanabe H, Koike Y, Kanaoke Y, Sakurai N, Hakusui Y, Takahashi A (1993) Treatment of postprandial hypotension with selective alpha 1 and beta 1 adrenergic agonists. J Auton Nerv Syst 45:149–154
12. Hokanson DE, Sumner DS, Strandness DE Jr (1975) An electrically calibrated plethysmograph for direct measurement of limb blood flow. IEEE Trans Biomed Eng 22:25–29
13. Jansen RW, Lipsitz LA (1995) Postprandial hypotension: epidemiology, pathophysiology, and clinical management. Ann Intern Med 122:286–295
14. Lipsitz LA, Fullerton KJ (1986) Postprandial blood pressure reduction in healthy elderly. J Am Geriatr Soc 34:267–270
15. Mathias CJ, Bannister R (1999) Investigation of autonomic disorders. In: Bannister R, Mathias CJ (eds) Autonomic failure. A textbook of clinical disorders of the autonomic nervous system, 4th ed. Oxford University Press, pp 171–175
16. Mathias CJ, da Costa DF, Fosbraey P, Bannister R, Wood SM, Bloom SR, Christensen NJ (1989) Cardiovascular, biochemical and hormonal changes during food-induced hypotension in chronic autonomic failure. J Neurol Sci 94:255–269
17. Mathias CJ, Holly E, Armstrong E, Shareef M, Bannister R (1991) The influence of food on postural hypotension in three groups with chronic autonomic failure—clinical and therapeutic implications. J Neurol Neurosurg Psychiatr 54:726–730
18. Micieli G, Martignoni E, Cavallini A, Sandrini G, Nappi G (1987) Postprandial and orthostatic hypotension in Parkinson's disease. Neurology 37:386–393
19. Norryd C, Dencker H, Lunderquist A, Olin T, Tylen U (1975) Superior mesenteric blood flow during digestion in man. Acta Chir Scand 141:197–202
20. Seyer-Hansen K (1977) Postprandial hypotension. Br Med J 2:1262
21. Smirk FM (1953) Action of a new methonium compound (M&B 2050A) in arterial hypertension. Lancet 1:457–464
22. Smith JJ, Kampine JP (1990) Blood and the ciuculation: general features. In: Smith JJ, Kampine JP (eds) Circulatory physiology, 3rd ed. Williams & Wilkins, pp 1–15
23. Stewart JM (2002) Pooling in chronic orthostatic intolerance: arterial vasoconstrictive but not venous compliance defects. Circulation 105:2274–2281
24. Svensson CK, Edwards DJ, Mauriello PM, Barde SH, Foster AC, Lanc RA, Middleton E Jr, Lalka D (1983) Effect of food on hepatic blood flow: implications in the "food effect" phenomenon. Clin Pharmacol Ther 34:316–323
25. Thomaides T, Bleasdale-Barr K, Chaudhuri KR, Pavitt D, Marsden CD, Mathias CJ (1993) Cardiovascular and hormonal responses to liquid food challenge in idiopathic Parkinson's disease, multiple system atrophy, and pure autonomic failure. Neurology 43:900–904
26. Yokota T, Kamata T, Mitani K (1997) Postprandial cerebral ischemia. Stroke 28:2322–2323